Titanium hydroamination catalysts bearing a 2-aminopyrrolinato spectator ligand: monitoring the individual reaction steps†

Katharina Weitershaus,[a] Benjamin D. Ward,[a] Raphael Kubiak,[b] Carsten Müller,[b] Hubert Wadepohl,[a] Sven Doye*[b] and Lutz H. Gade*[a]

Received 2nd February 2009, Accepted 25th March 2009
First published as an Advance Article on the web 15th April 2009
DOI: 10.1039/b902038a

A series of new titanium half sandwich complexes, containing a 2-aminopyrrolinato ligand $\{N^{Xyl}N\}^-$ as the ancillary ligand, have been prepared and are shown to be pre-catalysts for the hydroamination of alkynes. The coordination of $\{N^{Xyl}N\}^-$ to titanium was achieved by reaction of $[Cp^*TiMe_3]$ with the protioligand $N^{Xyl}NH$ giving $[Cp^*Ti(N^{Xyl}N)(Me)_2]$ (**1**). Upon reaction of complex **1** with an excess of *tert*-butylamine, the imido complex $[Cp^*Ti(N^{Xyl}N)(N^tBu)(NH_2{}^tBu)]$ (**2**) was formed. The latter provided the preparative entry to the synthesis of a range of *N*-aryl substituted imido complexes. Imido ligand exchange with 2,6-dimethylaniline, 2,4,6-trimethylaniline as well as 2,6-diisopropylaniline gave the corresponding arylimido complexes **3–5** in clean reactions. Reaction of the titanium imido complex $[Cp^*Ti(N^{Xyl}N)(N^tBu)(NH_2{}^tBu)]$ **2** with terminal arylacetylenes, such as phenylacetylene and tolylacetylene, led to C–H activation and the formation of alkynyl/amido complexes, whereas the arylimido complexes **3** and **5** cleanly underwent {2 + 2} cycloaddition, giving the azatitanacyclobutene derivatives. A single-crystal X-ray structure analysis of the azatitanacyclobutene $[Cp^*Ti(N^{Xyl}N)\{\kappa^2N(2,6\text{-}C_6H_3Me_2)CTol{=}CH\}]$ (**11**) provided the first crystallographically characterized Markovnikov cycloaddition product of an imidotitanium complex with a terminal alkyne. The mechanistic aspects of the hydromanination of alkynes with the new Ti half sandwich complexes were studied and established a reversible {2 + 2} cycloaddition step and the cleavage of the metallacyclic intermediate as the rate determining step in the catalytic cycle. The titanium half sandwich imido complexes were found to be active catalysts for the inter- and intramolecular hydroamination of a broad range of alkynes and ω-aminoalkynes.

Introduction

The development of catalytic methods for the hydroamination of non-activated alkenes, allenes and alkynes has received considerable attention in recent years.[1] These highly atom economic processes allow direct access to industrially and biologically relevant classes of compounds such as amines, enamines and imines from cheap and readily available starting materials. This has recently led to an ever increasing range of molecular compounds, which have been identified as catalysts for these transformations.[1] However, many of the newly developed processes are limited in their scope. Whereas rare earth catalysts have been found to be mainly active in intramolecular hydroamination, other catalysts—in particular those of the late transition metals—are frequently limited to the addition of weakly basic substrates (aniline, sulfonamides, carboxamides, *etc.*) to alkenes, alkynes and allenes.

Neutral group 4 metal complexes appear to possess a relatively broad scope. They have been employed for the intramolecular hydroamination of alkynes,[2] allenes[3] and alkenes[4] as well as the intermolecular hydroamination of alkynes[5] and allenes.[6] Primary aryl- and alkylamines have been successfully used, however, secondary amines have so far defied this type of transformation with neutral catalysts.[7] For the reactions of the latter, cationic Zr- and Ti-complexes have been employed in intramolecular cyclizations of aminoalkenes.[8]

Among all the varieties of aminations of C–C multiple bonds, the Ti-catalyzed hydroamination of alkynes,[2,5] which generally gives imines as reaction products has been the most intensely studied. The currently accepted mechanism is based on the assumption that—in analogy with the Zr-catalyzed transformation—an imidotitanium species is the active species.[6,9,10] The latter is formed from a suitable precursor complex, such as *e.g.* $[Cp_2TiMe_2]$ or a variety of other compounds, all of which have two formally anionic reactive ligands at the titanium (alkyl-, dimethylamide-, chloride-ligands), which are transformed to the Ti=N multiple bond in a first reaction step. Alternatively preformed imido complexes may be used as catalysts.

Apart from the choice of the appropriate "reactive" ligands at the group 4 metal centre, the control of its reactivity by the ancillary ligand(s) is crucial for the performance of the catalyst. In recent years, amidinates have been shown to be ideal ancillary ligands for a variety of early transition metals, including group 3

[a]*Anorganisch-Chemisches Institut, Universität Heidelberg, Im Neuenheimer Feld 270, 69120 Heidelberg, Germany. E-mail: lutz.gade@uni-hd.de; Fax: +49 6221 545 609*
[b]*Institut für Reine und Angewandte Chemie, Universität Oldenburg, Carl-von-Ossietzky-Str. 9–11, 26111 Oldenburg, Germany, doye@uni-oldenburg.de; Fax: +49 4417 983 329*

† Electronic supplementary information (ESI) available: Kinetic investigations. CCDC reference numbers 718799–718803. For ESI and crystallographic data in CIF or other electronic format see DOI: 10.1039/b902038a

and lanthanides,[11] as well as for metals from groups 4[12] and 5.[13] We have recently reported the synthesis of 2-aminopyrrolinato ligands in which the amidinato binding unit is exocyclic with respect to the heterocycle and which have proven to act as particularly robust spectator ligands.[14] Their use in the preparation of a series of new titanium half sandwich complexes, which are shown to be pre-catalysts for the inter- and intramolecular hydroamination of alkynes, will be reported in this work.

Results and discussion

Synthesis of titanium half sandwich complexes bearing a 2-aminopyrrolinato spectator ligand

The coordination of the 2-aminopyrrolinato ligand $\{N^{Xyl}N\}^-$ to titanium was achieved in a straightforward two-step procedure in which [Cp*TiMe$_3$] was generated *in situ* by reaction of [Cp*TiCl$_3$] with three equivalents of methyl lithium and subsequent reaction with the protioligand $N^{Xyl}NH$. The methane elimination is rapid and irreversible and, even in the presence of an excess of amidine, occurred only once giving selectively the dimethyl complex [Cp*Ti($N^{Xyl}N$)(CH$_3$)$_2$] (**1**) (Scheme 1).

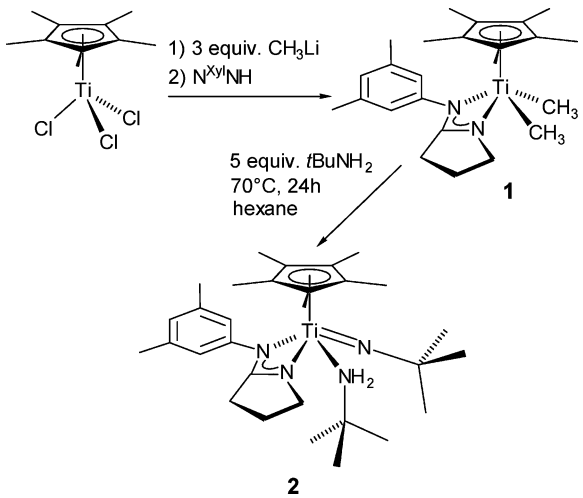

Scheme 1 Synthesis of [Cp*Ti($N^{Xyl}N$)(CH$_3$)$_2$] (**1**) and its aminolytic conversion to [Cp*Ti($N^{Xyl}N$)(N^tBu))($NH_2{}^t$Bu)] (**2**).

In the ^{1}H and ^{13}C NMR spectra of the dimethyl complex [Cp*Ti($N^{Xyl}N$)(CH$_3$)$_2$] (**1**), only one titanium-methyl resonance is observed indicating a dynamic behaviour ($\kappa^2 \Leftrightarrow \kappa^1$) (or possibly an in-place rotation) of the amidinato ligand, which we have previously observed for bis(amidinato)titanium complexes[14] and which has also been reported and discussed in detail for amidinatotitanium half sandwich compounds by Sita *et al.*[15] Variable low temperature ^{1}H NMR studies (400 MHz) established the coalescence point at −66 °C and a $\Delta G^{\neq}$ for the overall process of 40.9(±0.2) kJ mol^{-1}.

A single-crystal X-ray diffraction study of **1** confirmed the proposed piano stool coordination geometry of the complex in which the Cp*-ligand occupies the apical coordination site [Ti–Cp(centroid) 2.045 Å). Its molecular structure is depicted in Fig. 1 along with selected bond lengths and angles.

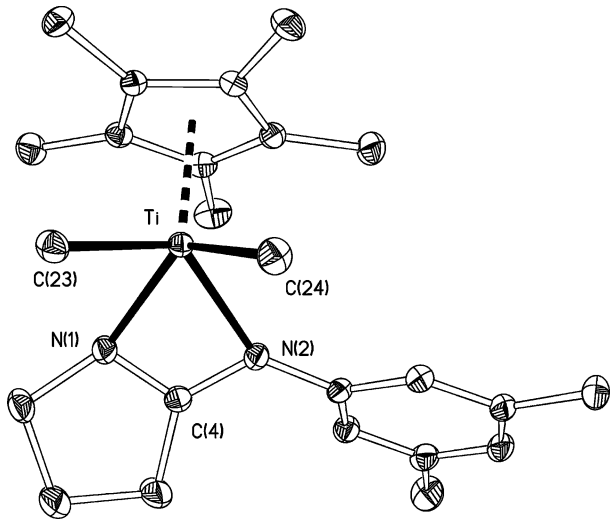

Fig. 1 Molecular structure of [Cp*Ti($N^{Xyl}N$)(CH$_3$)$_2$] (**1**). Hydrogen atoms are omitted for clarity (displacement ellipsoids set at 40% probability). Selected distances (Å) and angles (°): Ti–N(1) 2.127(1), Ti–N(2) 2.193(1), Ti–C(23) 2.136(1), Ti–C(24) 2.128(1), Ti–Cent. 2.045, N(1)–C(4) 1.315(2), N(2)–C(4) 1.331(2), N(1)–Ti–N(2) 61.72(5), C(23)–Ti–C(24) 88.11(6), N(1)–Ti–C(23) 81.66(6), N(2)–Ti–C(24) 90.57(6).

The bite angle of the κ^2-coordinated amidinato ligand was found to be 61.72(6)°, which is within the range of previously reported values for this type of ligand system (min: 59°, max: 67°, mean: 63°, for 92 titanium complexes bearing amidinato ligands),[16] and the Ti(1)–$N_{Amidinato}$ distances of 2.1269(13) and 2.1927(13) Å are also in the range of previously determined values (min: 1.953, max: 2.275 Å, mean: 2.112 Å, for 92 examples).[16]

Upon reaction of complex **1** with an excess of *tert*-butylamine, aminolyses occurs and the imido complex [Cp*Ti($N^{Xyl}N$)(N^tBu)($NH_2{}^t$Bu)] (**2**) is cleanly formed (Scheme 1). One molar equivalent of the amine is converted to the formally dianionic four-electron donor imido ligand whilst a second equivalent of tBuNH$_2$ coordinates to the metal as a neutral ligand. The *tert*-butyl substitutents can be distinguished and assigned based on the ^{13}C NMR chemical shifts of their quaternary carbon nuclei. The imido signal is detected at 67.1 ppm, whereas the corresponding nucleus of the amine resonates at 50.4 ppm. The high frequency shift of the quaternary C atom of the imido substituent is diagnostic for this structural unit.[17]

The two proton signals of the NH_2 group of the coordinated amine are very broad at 295 K but give two well resolved resonances at 218 K. The doublets of both protons are observed at 7.28 and 1.80 ppm, indicating a strong shielding anisotropy due to the aromatic rings in the molecule. The $^2J_{H-H}$ coupling constant of 11 Hz is as expected for geminal coupling.

Synthesis and structural characterization of arylimidotitanium complexes

It was not possible to substitute the coordinated *tert*-butylamine in **2** by direct reaction with other donor ligands such as pyridine or 4-dimethylaminopyridine (dmap). The amine could only be removed by reaction with the strong Lewis acid tris(pentafluorophenyl)borane (BArF). The reaction product, [Cp*Ti($N^{Xyl}N$)(N^tBu)] (**2a**), was found to be stable

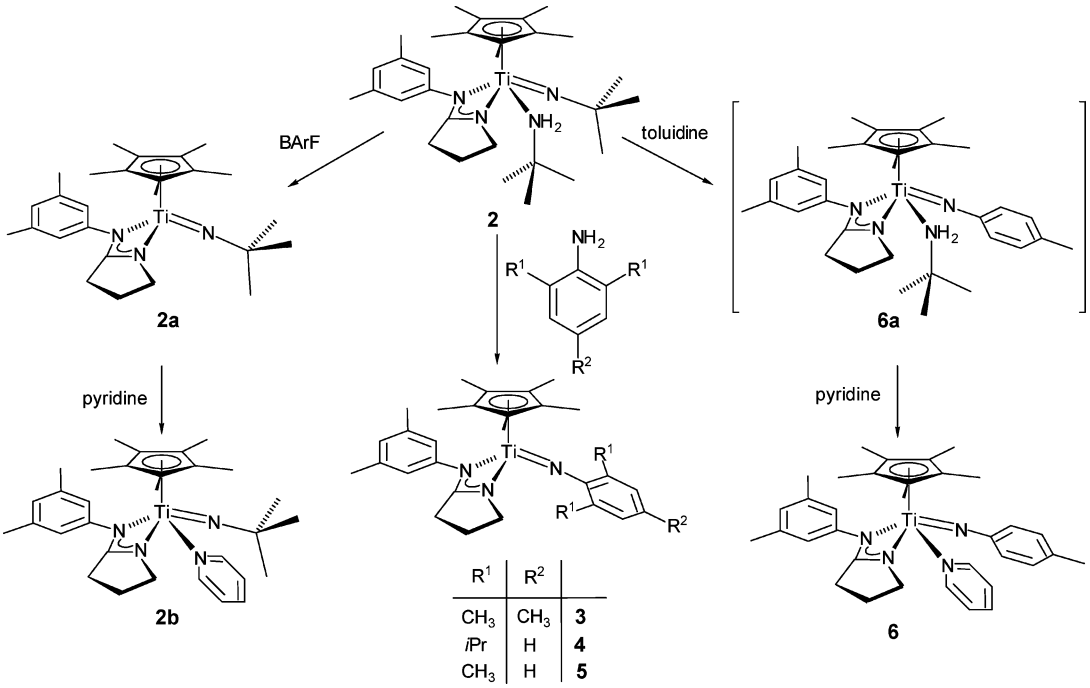

Scheme 2 Imide exchange reactions of [Cp*Ti(N^{Xyl}N)(N^{t}Bu)($NH_2{}^{t}$Bu)] (**2**) for the synthesis of arylimido complexes.

in solution and could be characterized by NMR spectroscopy. By addition of pyridine to **2a** the corresponding donor-adduct [Cp*Ti(N^{Xyl}N)(N^{t}Bu)(py)] (**2b**) was obtained quantitatively (Scheme 2).

Complex **2** provided the preparative entry to the synthesis of a range of *N*-aryl substituted imido complexes. Such imido exchange reactions have been reported and extensively exploited by Mountford and co-workers.[18] Imido ligand exchange with 2,6-dimethylaniline, 2,4,6-trimethylaniline as well as the sterically demanding 2,6-diisopropylaniline gave the corresponding imido complexes **3–5** in clean reactions (Scheme 2). As a consequence of the steric bulk of the 2,6-aryl substituents on the imides, all of the compounds were isolated without additional coordinated amine. All three complexes are green diamagnetic solids for which single crystals could be obtained from hexane solutions. Since only crystals of poor quality were obtained for complex **5** the metric parameters of this structure are to be viewed with some caution. However, its gross structural features are well established and will be related to those of compounds **3** and **4** which are discussed in detail.

Compounds **3–5**, which are displayed in Fig. 2, are piano stool sandwich complexes. The imido-N–titanium bond lengths of 1.736(1) Å (**3**) and 1.738(1) Å (**4**) are in the range which has been previously reported for imidotitanium complexes with ancillary amidinato ligands (min: 1.656 Å, max: 1.752 Å, mean: 1.712 Å, for 14 examples in the CSD). The same applies to the amidinato-N–Ti distances of 2.091(1) Å and 2.106(1) Å for **3** and 2.082(12) Å and 2.115(1) Å for complex **4**. The bond angle Ti–N(3)–C(13) of 168.5(1)° in **3** deviates significantly from linearity. This distortion is even more pronounced in complex **4** [164.9(1)°] and is attributed to the steric repulsion between the isopropyl groups on the imido substituent and the 3,5-xylyl moiety on the amidinato ligand. Despite the bending of the imides they are nevertheless to be viewed as 4-electron donors which render the half sandwich species overall 16 valence electron complexes.[19]

If a sterically less crowded aromatic amine such as *para*-toluidine is employed in the imide exchange, only the *tert*-butyl imido ligand is exchanged whilst the additional molecule of *tert*-butylamine remains coordinated to the titanium centre (Scheme 2). The resulting complex (**6a**) was not isolated and only characterized in situ by NMR spectroscopy. By addition of one molar equivalent of pyridine the coordinated *t*-BuNH_2 is substituted and the resulting complex **6** was isolated as an orange solid. The *ortho*-protons of the coordinated pyridine in **6** are observed at 8.74 ppm, which is characteristically shifted to higher frequency compared to free pyridine.[20]

Reactions of imido complexes with terminal alkynes: C–H activation *vs.* {2 + 2} cycloaddition

Reaction of the titanium imido complex [Cp*Ti(N^{Xyl}N)(N^{t}Bu)($NH_2{}^{t}$Bu)] (**2**) with terminal arylacetylenes, such as phenylacetylene and tolylacetylene, led to C–H activation and the formation of alkynyl/amido complexes **7** and **8** (Scheme 3, top). The conversion is rapid and irreversible. The coordinated *tert*-butylamine in **2** is displaced and a proton is transferred from the terminal acetylene to the imido nitrogen atom.

Competing C–H-activation and {2 + 2}-cycloaddition reactions have been previously reported by Bergman[21] and by us.[22] We also note that C–H-activations induced by group 4 metal imides in general have been extensively studied by Wolczanski,[23] Bergman[24] and Scott.[5n]

The newly formed [NH-*t*Bu]$^-$ ligand could be detected by ^{15}N-NMR spectroscopy and resonates at 331 ppm whilst the signal of the imido nitrogen atom of the reactant was observed at 407 ppm. The assignment is backed up by ^{15}N-HMBC spectra, the $^1J(^{15}N–^1H)$ coupling constant in the NH-unit of **7** and **8** is 63 Hz. In contrast to the observed reactivity of the alkyl substituted imido complex **2**, the arylimido complexes **3** and **5** cleanly underwent

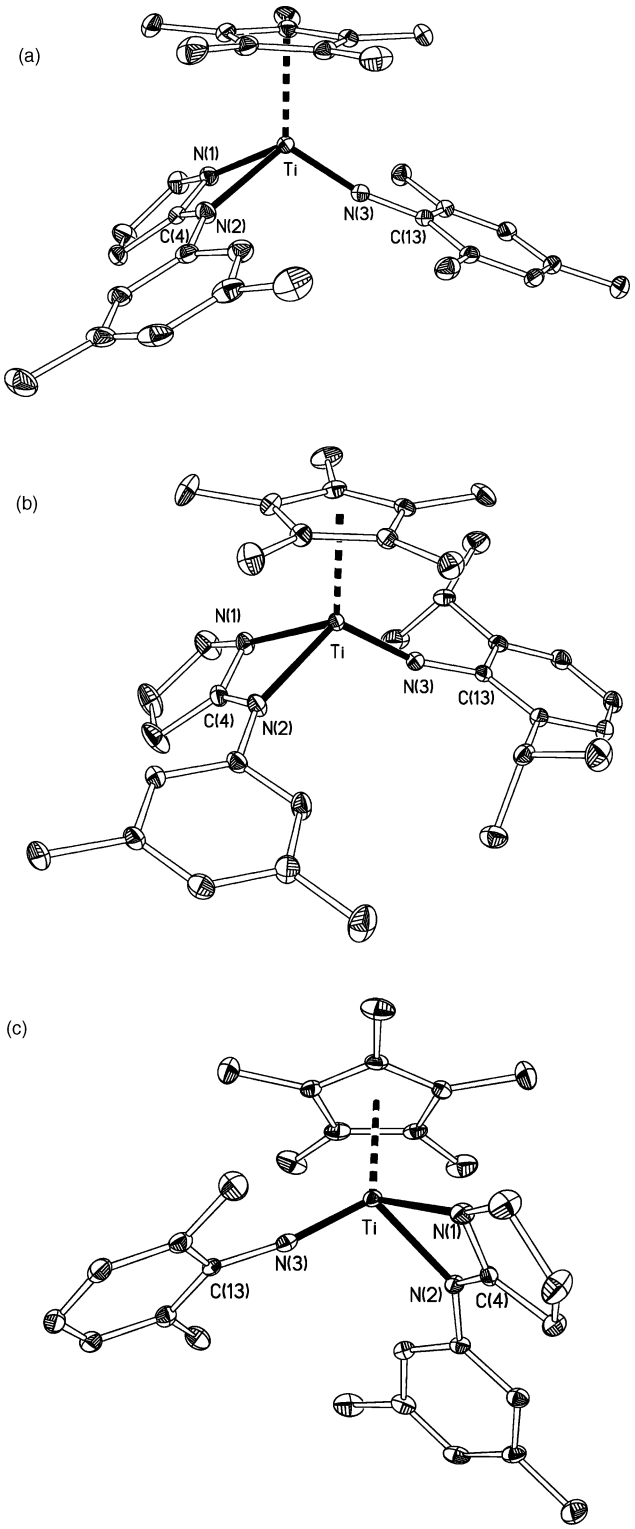

Fig. 2 Molecular structures of the aryl imidocomplexes. (a) [Cp*Ti(N^{Xyl}N)(2,4,6-$NC_6H_2Me_3$)] (**3**), (b) [Cp*Ti(N^{Xyl}N)(2,6-NC_6H_3-(^iPr)$_2$)] (**4**), (c) [Cp*Ti(N^{Xyl}N)(2,6-$NC_6H_3Me_2$)] (**5**). Hydrogen atoms are omitted for clarity (displacement ellipsoids set at 40% probability). Selected bond lengths (Å) and angles (°) of all three complexes are listed in Table 1.

{2 + 2} cycloaddition giving the azatitanacyclobutene derivatives **9–11** (Scheme 3), which are postulated as intermediates in the catalytic cycle of the hydroamination of alkynes. Reaction of the

Table 1 Selected bond distances (Å) and angles (°) for imido compounds (**3**), (**4**) and (**5**)

	3	**4**	**5**
Ti–N(1)	2.091(1)	2.082(1)	2.084(3)
Ti–N(2)	2.106(1)	2.115(1)	2.105(3)
Ti–N(3)	1.736(1)	1.738(1)	1.728(3)
Ti–cent.	2.042	2.038	2.036
N(3)–C(13)	1.381(2)	1.378(2)	1.381(5)
N(1)–C(4)	1.324(2)	1.327(2)	1.319(5)
N(2)–C(4)	1.339(2)	1.332(2)	1.335(5)
N(1)–Ti–N(2)	64.25(5)	64.74(5)	64.3(1)
Ti–N(3)–C(13)	168.5(1)	164.9(1)	170.6(3)

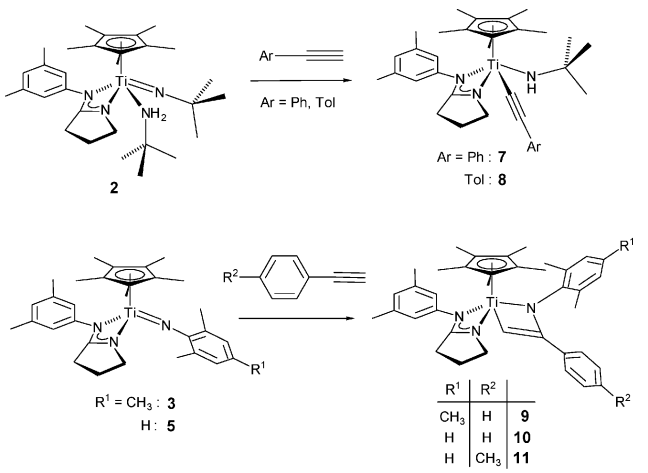

Scheme 3 Reactions of imidocomplexes with terminal alkynes: C–H activation for **2** *vs.* {2 + 2} cycloaddition for **3** and **5**.

arylimides with two molar equivalents of alkyne for four hours at ambient temperature gave complete conversion to complexes **9–11**. Bulky substituents in the *ortho* positions of the aromatic substituent of the imido ligand partially suppressed the cycloaddition, as in the case of complex **4**, for which only partial conversion to a metallacyclic product was observed in the NMR tube.

In situ ^{1}H-NMR studies of the {2 + 2} cycloadditions depicted in Scheme 3 revealed the formation of only one of the two possible regioisomers. The ^{1}H NMR signal of the methyne proton on the metallacycle was observed at high frequency (11.1 ppm) for all three derivatives. The corresponding resonances for metallacycles leading to the anti-Markovnikov products have been previously observed shifted by 1–2 ppm to lower frequency.[25] In order to establish the details of the molecular structure of the metallacyclic reaction products, a single-crystal X-ray structure analysis of compound **11** has been carried out. Its molecular structure is depicted in Fig. 3 along with the principal bond lengths and angles. To our knowledge, complex **11** is the first crystallographically characterized Markovnikoff cycloaddition product of an imidotitanium complex with a terminal alkyne.

The coordination geometry at the metal centre may be described as a four-legged piano stool with a Ti-Cp*–cent distance of 2.048 Å. The Ti–N(1) bond length of the amidinate of 2.203(2) Å is slightly greater than in previous examples whilst the Ti–N(2) distance has remained essentially unaffected. The slightly non-symmetrical coordination of the amidinato ligand compared to the situation in **1**, **3** and **5** may be attributed to greater steric

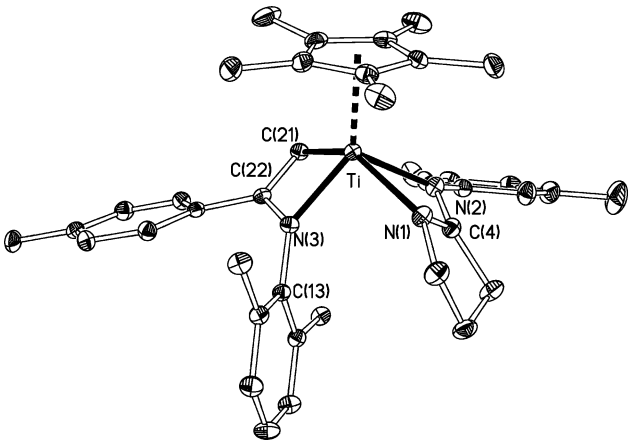

Fig. 3 Molecular structure of [Cp*Ti(N^{Xyl}N){κ^2N(2,6-$C_6H_3Me_2$)-CTol=CH}] (**11**). Hydrogen atoms are omitted for clarity (displacement ellipsoids set at 40% probability; only the prevailing conformation of the C_4N ring is shown). Selected bond lengths (Å) and angles (°): Ti–N(1) 2.203(2), Ti–N(2) 2.095(2), Ti–N(3) 1.959(2), Ti–C(21) 2.051(2), C(21)–C(22) 1.349(2), C(22)–N(3) 1.424(2), Ti-Cent 2.048, N(1)–C(4) 1.309(2), N(2)–C(4) 1.337(2), C(21)–Ti–N(3) 70.35(7), N(1)–Ti–N(2) 62.16(6), N(3)–Ti–N(1) 87.51(6), N(2)–Ti–C(21) 94.24(7).

crowding by the metallacycle, compared with the almost linear imido ligand. The deviation from symmetrical binding is also reflected in the N(1)–C(4) and N(2)–C(4) bond lengths, which were found to be 1.309(2) and 1.337(2) Å, respectively.[26] As for the metric parameters of the metallacycle, the Ti–N(3) distance of 1.959(2) and the Ti–C(21) bond length of 2.051(2) Å indicate single bonds whereas the C(21)–C(22) distance of 1.349(2) Å is consistent with there being a carbon–carbon double bond.[20,22] This interpretation has been recently confirmed by a DFT study of a related azatitanacyclobutene derivative.[20] To minimize the intra- and inter-ligand repulsion, the 2,6-xylyl substituent on the metallacycle adopts an orthogonal orientation with respect to the plane of the four-membered ring.

$$[\text{imide}] + [\text{acetylene}] \rightleftharpoons [\text{metallacycle}] \quad K = \frac{[\text{metallacycle}]}{[\text{imide}][\text{acetylene}]}$$

The metallacyclobutene is in equilibrium with the starting materials, the imido complex and phenylacetylene. With increasing temperature the equilibrium is shifted towards the latter. Van't Hoff analysis of the equilibrium constants determined between 45 °C and 70 °C permitted the determination of the thermodynamics of this equilibrium (Fig. 4). ΔS_o was obtained as -173 ± 6 J mol^{-1} K^{-1} and ΔH_o as -64 ± 4 kJ mol^{-1}.

A DFT study of the reactions of the imido complexes with alkynes

The observed selectivity with regard to cycloaddition *vs.* C–H activation is apparently dependent on the imido *N*-substituent. In light of this, we sought to rationalise this selectivity by considering the reaction product and transition state structures for both of these reaction pathways, which were modelled using DFT (B3PW91) methods. Unfortunately, calculations of complexes possessing these amidinate ligands have a tendency to have poorly defined minima on the potential energy surface;[14] the reaction products were calculated on both simplified systems and on the non-simplified models, however well-defined transition states could

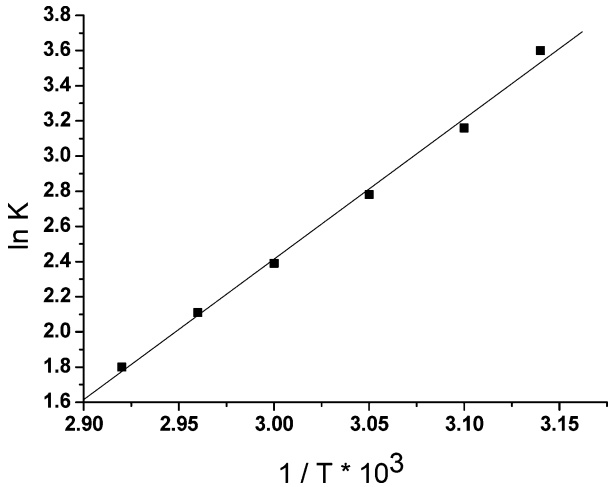

Fig. 4 The thermodynamics of the equilibrium between the imide **5** and acetylene and the metallacyclic compound **10** determined by Van't Hoff analysis of the equilibrium constants between 45 °C and 70 °C.

only be located when the simplified system [CpTi(NMe)(lig_{qm})] **A** was employed.

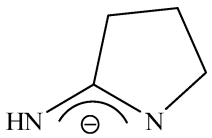

lig_{qm}

An analysis of the metric parameters of the reaction products with the non-simplified system indicates no significant differences with those using the simplified system (*e.g.* T=N = 1.678 Å for **A** and 1.681 Å for [Cp*Ti(N^{Xyl}N)(N^tBu)] **2a** modelled with the same method), but in the absence of transition states for the more complex model, our discussion is confined to the simplified system.

An energy profile diagram is shown in Fig. 5, with the C–H activation pathway leading to the acetylide product **B** *via* transition state **B**‡, and the cycloaddition product **C** *via* transition state **C**‡. Both the acetylide **B** and titanacyclobutene **C** are viable products, with the cycloaddition product **C** being thermodynamically more favourable. With this simplified system, the cycloaddition pathway has the lowest activation barrier, 3.5 kcal mol^{-1}, compared to the acetylide formation, which has an activation barrier of 9.3 kcal mol^{-1}.

Even when allowing for the error in the calculation methods, this relatively small difference in transition state energies indicates that the cycloaddition pathway is implicated as both the thermodynamically, as well as the kinetically favoured pathway. Therefore in the absence of any extenuating circumstances arising from the additional complexity of the 'real' system, compared to the model system, it would be expected that the reaction of these imido complexes with acetylenes would yield solely the cycloaddition product. Although the 'real' models did not give rise to well defined minima on the potential energy surface, the selectivity can be easily rationalised by a closer inspection of the transition state structures **B**‡ and **C**‡, which are also illustrated in Fig. 5. When considering steric arguments, it can be seen that in the C–H activation transition state **B**‡, the non-reacting acetylene

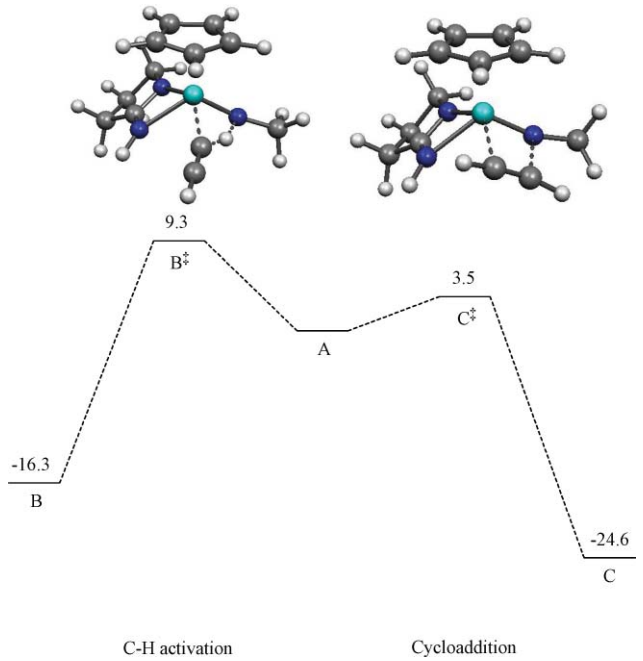

Fig. 5 Energy profile for the reaction of the computational model [CpTi(lig$_{qm}$) (NMe)] (**A**) with acetylene (kcal mol^{-1}). The calculated transition state structures for C–H activation (**B**‡) and cycloaddition (**C**‡) of **A** with acetylene are also depicted.

C–H (which would represent the alkyl or aryl substituent in terminal acetylenes) is directed away from both the imido *N*-substituent and the amidinate aryl group (represented by a proton in the model system). It would therefore be expected that the transition state energy would be influenced little, if at all, by altering the acetylene or imido substituents.

Conversely with the cycloaddition transition state structure **C**‡, the two acetylene protons are both in close proximity to other co-ligands; one of them is in close proximity to the amidinate N–H, which in the real system would be replaced by an aryl group. The remaining acetylene C–H lies in close proximity to the imido substituent. It can be clearly seen from the molecular structure shown in Fig. 5 that there is insufficient space for an acetylene substituent to be located close to the aromatic amidinate substituent, thereby forcing any acetylene substituent to reside close to the imido substituent. It is therefore expected that the relative energy of this transition state will be strongly dependent on the steric repulsion between these two groups; larger acetylene substituents coupled with larger imido substituents will increase the energy of the corresponding transition state. Since, as noted above, the cycloaddition pathway possesses the lowest activation barrier by only a relatively small amount, any increase in the steric repulsion between these two groups will reduce the difference between the relative activation energies of the two possible pathways, especially since we have noted that the transition state energy of **B**‡ will remain largely unaffected by alterations in either of these groups. It is perhaps unsurprising therefore that in the real system, the smaller aryl imido complex undergoes the expected cycloaddition reaction, whereas in the significantly larger *tert*-butyl imido complex favours the C–H activation pathway due to a destabilisation of the cycloaddition transition state.

In addition to explaining the role of the imido substituent in the cycloaddition *vs.* C–H activation selectivity, the cycloaddition transition state **C**‡ also shows, as alluded to above, that the most stable arrangement in the 'real' system is that in which the acetylene substituent is located closest to the imido substituent, and hence furthest from the amidinate aryl substituent, since the amidinate substituent reduces the longitudal space in that direction of the amidinate, relative to the orientation of the acetylene in the cycloaddition transition state. The greater feasibility of this transition state implies that catalytic hydroamination reactions using terminal alkynes will be more favoured in the Markovnikov sense, rather than the anti-Markovnikov; this relative stability is readily inferred by a consideration of the catalysis studies (*vide infra*), in which selectivities of 99 : 1 are observed.

A kinetic analysis of the key steps in the catalytic hydroamination cycle

The active species in the generally accepted catalytic cycle for the hydroamination of alkynes is an imido-transition metal complex.[6,9,10] We studied the mechanistic aspects of our catalysts for the reaction of complex **5** with phenylacetylene since it proved to be possible to isolate the first proposed intermediate in the catalytic cycle, the azatitanacyclobutene complex **10**. As discussed above, this first {2 + 2} cycloaddition step was found to be reversible, the metallacycle being in equilibrium with the imide and the acetylene starting materials. In Scheme 4, the cycloaddition and cycloreversion are characterized by the rate constants k_1 and k_{-1}. In the presence of primary amine the metallacyclic compound **10** may undergo aminolysis to generate a diamido intermediate, which rapidly forms the imido compound and liberates the reaction product. The intermediate diamido compound could never be observed by spectroscopic techniques, so that the disappearance of the metallacycle in the aminolysis is characterized by the second order rate law (rate constant k_2).

The individual equations for the generation and conversion of the metallacyclic intermediate **10** are given by:

$$[\text{imide}] + [\text{acetylene}] \underset{k_{-1}}{\overset{k_1}{\rightleftharpoons}} [\text{metallacycle}]$$

$$[\text{metallacycle}] + [\text{xylylamine}] \xrightarrow{k_2} [\text{enamine}] + [\text{imide}]$$

Overall, the rate of formation and disappearance of the metallacycle **10** (MC) is given by:

$$\mathrm{d[MC]}/\mathrm{d}t = k_1[\mathrm{I}][\text{acetylene}] - k_{-1}[\mathrm{MC}] - k_2\,[\mathrm{MC}][\text{amine}] \quad (1)$$

The formation and degradation of the metallacycle by cycloreversion as well as its aminolysis were investigated separately. For the cycloaddition and the determination of the rate constant k_1 only the first term in eqn (1) had to be considered since the reverse reaction, of the metallacycle does not play a significant role at temperatures below 10 °C. Moreover, at the beginning there was practically no cycloaddition product and thus the reverse reaction could be neglected. In our investigations we first proved that the formation of the metallacyclic compound **10** is in first order in both starting materials (method of initial rates). Therefore the imidotitanium compound **5** was reacted with 0.5, 1, 2, 3 and 5 molar equivalents of phenylacetylene and the conversion was monitored by ^{1}H NMR spectroscopy. The initial

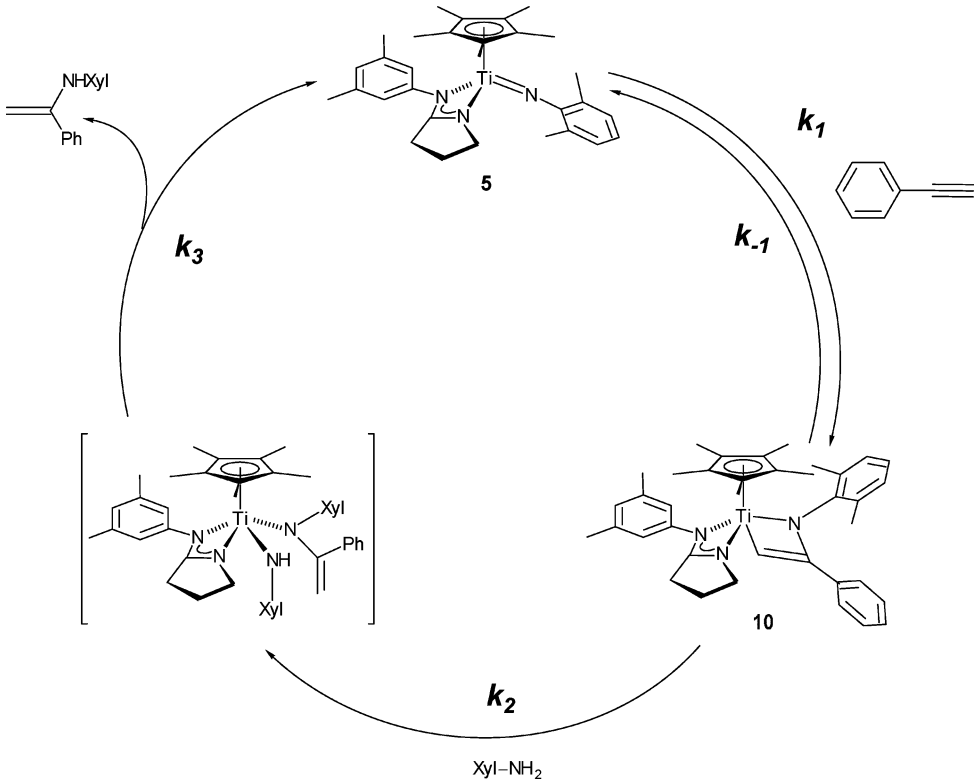

Scheme 4 Catalytic cycle of the hydroamination of phenylacetylene with 2,6-xylylamine using **5** as catalyst. The primary product of the aminolysis step following the {2 + 2} cycloaddition is not observed.

rates were plotted against the concentration of acetylene to give a linear dependence. (Fig. S1 in the ESI).† Subsequently, variable quantities of the imidotitanium compound **5** (5 to 25 μmol) were reacted with an excess (20 equiv.) of phenylacetylene. Using again the method of initial rates, a first order behaviour with respect to the concentration of the imido comlex **5** was found (Fig. S2 in the ESI).† The second order rate constant k_1 was then obtained by reacting equimolar amounts of imidotitanium compound with phenylacetylene (20 μmol). The reactions were monitored for several temperatures between 0 °C and 10 °C, giving the Arrhenius activation energy (Fig. 6). This measure was taken to suppress the cycloreversion which operates at higher temperature and allowed the extrapolation the rate coefficient k_1 for the reaction at 20 °C as 1.13×10^{-2} L mol^{-1} s^{-1}.

All other reaction steps were studied at 20 °C, because the cycloreversion and the aminolysis were impractically slow to monitor beneath 10 °C. Since we were able to isolate the metallacyclic complex **10**, the reverse reaction, which regenerates the reactants of the first step and the aminolysis could be studied separately. It was thus possible to neglect the rate of formation of **10**, since no imido complex was present at the beginning of the conversion and allowed the simplification of eqn (1), which assumes the following form:

$$-\mathrm{d[MC]}/\mathrm{d}t = k_{-1}[\mathrm{MC}] + k_2[\mathrm{MC}][\mathrm{amine}] \quad (2)$$

The rate of the cycloreversion displayed a first order dependence on the concentration of the metallacycle **10** (Fig. 7), which was proven by analysis of the initial rates. Therefore 5 to 25 μmol of the metallacyclic compound **10** were dissolved in benzene and

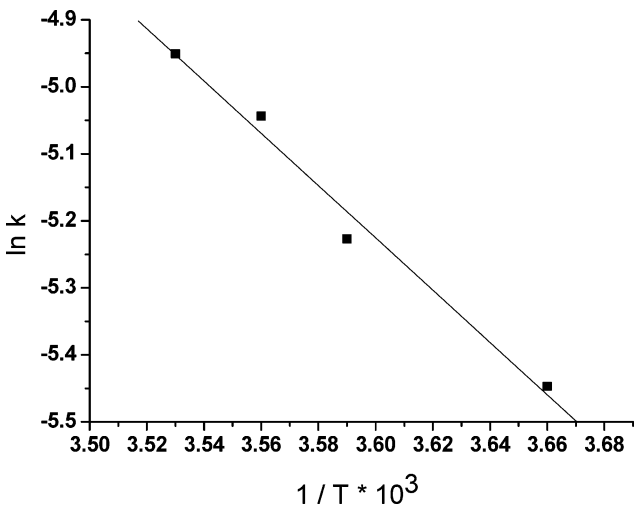

Fig. 6 Arrhenius plot for the cycloaddition leading to the metallacyclic compound **10** between 0 °C and 10 °C; determination of the temperature dependence of the rate constant k_1.

the disappearance of the compound was monitored by ^{1}H NMR spectroscopy. The initial rates were plotted *vs.* the concentration of complex **10** and from the straight line the rate coefficient k_{-1} was obtained as 3.4×10^{-5} s^{-1}.

The protolytic cleavage of the metallacycle **10** was found to obey the expected rate law which is first order in complex **10** (Fig. S3 in ESI)† as well as first order in the arylamine (Fig. 8). The straight line in Fig. 8 does not intersect the ordinate at the origin due to the competing cycloreversion reaction. The second order rate

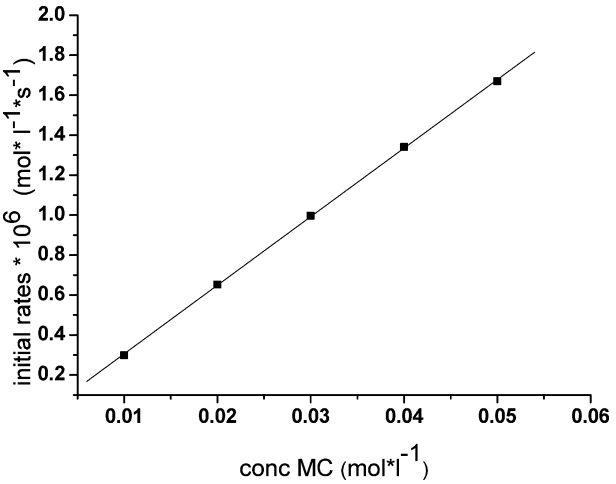

Fig. 7 Determination of the first order dependence on the concentration of the cycloreversion of the metallacyclic compound **10**. The analysis is based on the initial rates.

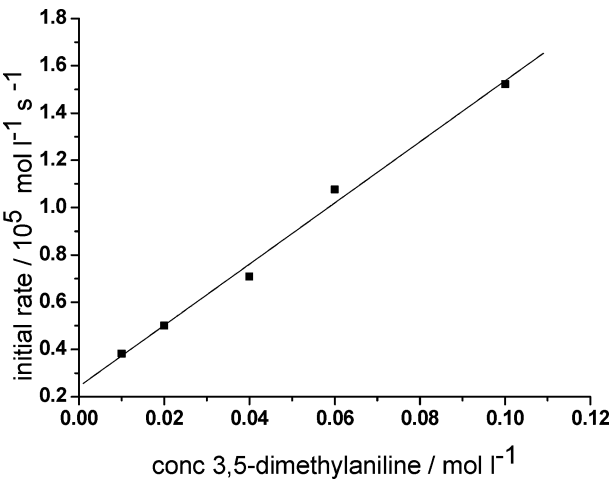

Fig. 8 First order dependence of the aminolysis of **10** on the concentration of arylamine. The analysis is based on the initial rates.

constant k_2 for the aminolysis was determined by eqn (3) as 1.58×10^{-3} L mol^{-1} s^{-1}.

$$-\mathrm{d[MC]}/\mathrm{d}t = k_{-1}[\mathrm{MC}] + k_2'[\mathrm{amine}] \text{ with } k_2' = k_2[\mathrm{MC}] \qquad (3)$$

The formation of the metallacyclic compound **10** by the imide **5** and phenylacetylene is thus faster by a factor of 7 than the aminolysis under the reaction conditions. The cleavage of the metallacyclic compound **10** by an arylamine is the rate determining step in this catalytic cycle as has been previously observed for this type of transformation.

The use of the titanium half sandwich imido complexes as pre-catalysts in the intermolecular hydroamination of alkynes

Pre-catalysts for the hydroamination of alkynes should be active for a broad range of substrates, easily synthetically accessible and convertible into imido complexes since they are the active species. Moreover, the ligand exchange reaction associated with the generation of the active catalyst should not interfere in the subsequent catalytic transformations. Finally, the catalysts should tolerate the elevated temperatures required for the hydroamination of some of the substrates.

Table 2 Intermolecular hydroamination of symmetric alkynes

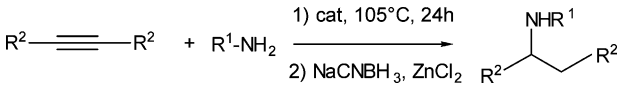

Entry	Alkyne	Amine	Cat.	Isolated yield (%)
1	Ph—≡—Ph	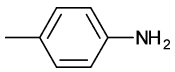	1	96
2			2	94
3	Ph—≡—Ph	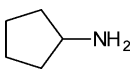	1	94
4			2	96
5	Ph—≡—Ph	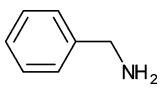	1	29
6			2	68
7	Ph—≡—Ph	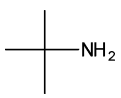	1	81
8			2	84
9	Ph—≡—Ph	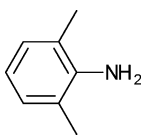	1	8
10			2	9
11	Ph—≡—Ph	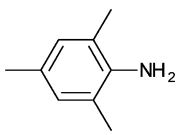	1	9
12			2	9
13		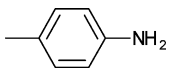	1	<5
14			2	<5

Reaction conditions: alkyne (2.4 mmol), amine (2.4 mmol), 5 mol% catalyst, 1 mL of toluene, 105 °C, 24 h. Reduction: $NaCNBH_3$ (4.8 mmol), $ZnCl_2$ (2.4 mmol), 10 mL methanol, 20 °C, 20 h. All yields determined after purification by column chromatography.

We therefore initially focused on the dimethyl complex **1** and the imido complex **2** in our study of the catalytic performance of the Ti half sandwich compounds reported in this paper. The methyl groups in **1** are readily and irreversibly cleaved by aminolysis with the primary amine giving the key imido species, which is preformed in complex **2**, making a specific activation step for the latter unnecessary. Furthermore, our studies of the stoichiometric reactivity of **2** delineated above indicated its facile convertibility to other imido derivatives. The *tert*-butylamine liberated in the latter process is volatile and remains only partially dissolved at the elevated temperatures (105 °C) employed in the catalytic runs.

The hydroamination of diphenylacetylene has been achieved with both primary aryl amines (entries 1 and 2 in Table 2) as well as alkyl amines (entries 3 and 4, 7 and 8, Table 2) with high isolated yields. Only the sterically crowded amines, 2,6-dimethylaniline (entries 9 and 10, Table 2) and 2,4,6-trimethylaniline (entries 11 and 12, Table 2) gave rise to poor conversion. The two pre-catalysts **1** and **2** did not give rise to any differences in activity, except for the hydroamination of diphenyacetylene with benzylamine (entries 5

Table 3 Intermolecular hydroamination of 1-phenylpropyne

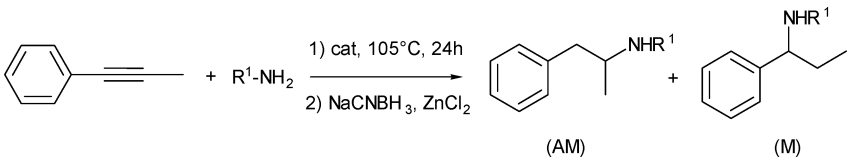

Entry	Alkyne	Amine	Cat.	Isolated yield (%)	Ratio AM : M
1	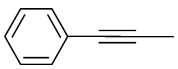	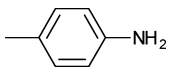	1	92	2 : 1
2			2	99	2 : 1
3	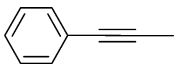	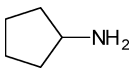	1	78	1 : 2
4			1	11	1 : 1.5
5	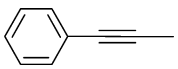	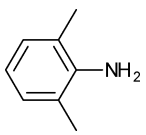	1	11	1 : 99
6			2	11	1 : 99
7	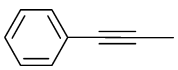	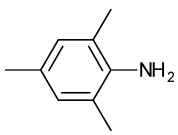	1	12	1 : 99
8			2	13	1 : 99

Reaction conditions: alkyne (2.4 mmol), amine (2.4 mmol), 5 mol% catalyst, 1 mL of toluene, 105 °C, 24 h. Reduction: $NaCNBH_3$ (4.8 mmol), $ZnCl_2$ (2.4 mmol), 10 mL methanol, 20 °C, 20 h. All yields determined after purification by column chromatography.

and 6). In this case, the *tert*-butylimido complex **2** displayed higher activity than complex **1**.

The limitations of this system became apparent in the hydroamination of 3-hexyne with *p*-toluidine (entries 13 and 14, Table 2). Even after a reaction time of 24 h at 105 °C no conversion was observed and it appears that the catalyst at hand is unsuitable for internal aliphatic alkynes.

On the other hand, in their use in the catalytic hydroamination of phenylpropyne both catalysts again display very similar activities and low regioselectivity with sterically undemanding amines. Whereas hydroamination with *p*-toluidine (entries 1 and 2, Table 3) preferentially yields the anti-Markovnikov product, the product ratio is completely inverted in the corresponding reaction with cyclopentylamine (3 and 4 in Table 3). This trend is enhanced for amines with increasing steric bulk, such as 2,6-dimethylaniline (entries 5 and 6) and 2,4,6-trimethylaniline (7 and 8 in Table 3), for which the Markovnikov products were obtained quantitatively.

In order to test a possible significance of the nature of the imido ligand in the performance of the catalyst we also investigated the hydroamination of terminal alkynes with the other imido complexes **3**, **4**, **5** and **6** and their corresponding primary amines. In the reaction of phenylacetylene with primary amines no significant differences in activity and selectivity was observed for these systems. Only for the coupling of 2,6-dimethylaniline with phenylacetylene (Table 4, entries 8, 9 and 10) complex **5** was found to be less selective with respect to the Markovnikov products than the reference systems **1** and **2**. Generally, the trend already established for 1-phenylpropyne was confirmed, that the regioselectivity is enhanced with increasing steric demand of the amines (a notable exception is the reaction with benzylamine which occurs with very high regioselectivity: entries 6 and 7, Table 4). Increasing the steric bulk beyond a certain point may lead to a loss in catalytic activity as has been shown for 2,6-diisopropylaniline (entry 12, Table 4). This behaviour is also reflected in the stoichiometric reactions of complex [Ti(N^{Xyl}N)(N-2,6-$C_6H_3{}^iPr_2$)] **4** with phenyl- and tolylacetylene which did not lead to detectable quantities of the corresponding azatitanacyclobutenes. It therefore seems to be at this step of the catalytic cycle that the reaction is suppressed.

Upon replacement of phenylacetylene by a terminal aliphatic alkyne such as 1-octyne, even 2,6-diisopropylaniline may be coupled in moderate yield (Table 5, entry 12). The steric demand of the amine leads to a high regioselectivity in this case. In general, 1-octyne was found to be more reactive as terminal alkyne than phenylacetylene also giving rise to generally higher selectivity of the hydroamination products (entries 1–3 and 6–12 in Table 5). The only exception to this trend is benzylamine for which both yield and regioselectivity in its reactions with 1-octyne are lower than for phenylacetylene (entries 4 and 5, Table 5).

Intramolecular hydroaminations of ω-aminoalkynes

Both complexes **1** and **2** have displayed excellent activities in the intramolecular hydroamination of several ω-aminoalkynes as is shown in Table 6. After reduction of the primary hydroamination products, the 2-benzyl-substituted piperidine derivatives were isolated in high yields.

Conclusions

The introduction of the 2-aminopyrrolinate as second ancillary ligand in Cp* titanium half sandwich complexes has allowed the

Table 4 Intermolecular hydroamination of phenylacetylene with primary amines

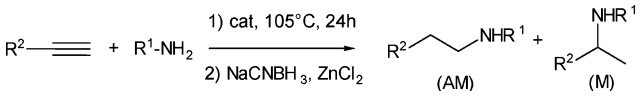

Entry	Alkyne	Amine	Cat.	Isolated yield (%)	Ratio AM : M
1	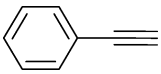	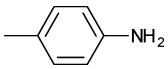	1	94	1 : 9
2			2	93	1 : 7
3			6	94	1 : 12
4	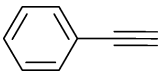	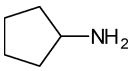	1	<5	—
5			2	<5	–
6	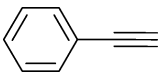	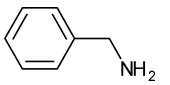	1	79	1 : 99
7			2	80	1 : 99
8	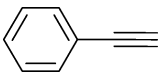	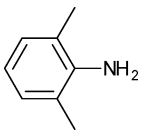	1	76 imine[a]	1 : 99
9			2	75 imine[a]	1 : 99
10			5	86[b]	1 : 13
11	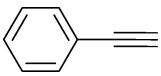	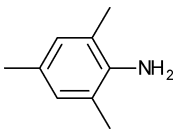	3	80 imine[a]	0 : 100
12	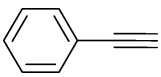	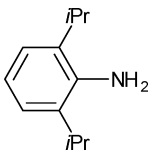	4	4	—

Reaction conditions: alkyne (2.4 mmol), amine (2.4 mmol), 5 mol% catalyst, 1 mL of toluene, 105 °C, 24 h. Reduction: $NaCNBH_3$ (4.8 mmol), $ZnCl_2$ (2.4 mmol), 10 mL methanol, 20 °C, 20 h. All yields determined after purification by column chromatography.[a] Reduction incomplete. Isolation of the imine. [b] Reduction with $LiAlH_4$.

isolation of key intermediates of the catalytic hydroamination of alkynes. On the other hand, these complexes have displayed good activities in the catalytic reactions themselves. Using sterically demanding amines as substrates excellent regioselectivities were observed in these transformations. Both the imido pre-catalyst **2** as well as the dimethyl precursor **1** display very similar activities and selectivities, indicating the role of the former itself as a key intermediate in the catalytic reaction.

Experimental

All manipulations of air and moisture sensitive species were performed under an atmosphere of argon using standard Schlenk and glove box techniques. Solvents were pre-dried over molecular sieves and dried over Na/K alloy (pentane, diethylether), Na (toluene) or K (THF, hexanes), distilled and stored over potassium mirrors in Teflon valve ampoules. Deuterated solvents were dried over K (benzene-d_6, toluene-d_8) vacuum distilled, and stored under argon in Teflon valve ampoules. [Cp*$TiCl_3$] was prepared according to a literature procedure.[27] The protioligand $N^{Xyl}NH$ was prepared as we have previously described.[14] Amines were dried over CaH_2, vacuum distilled and stored in Teflon valve ampoules before use. All other reagents were purchased from commercial suppliers and used as received unless otherwise stated. Samples for NMR spectroscopy were prepared under argon in 5 mm Wilmad tubes equipped with J. Young Teflon valves. NMR spectra were recorded on Bruker Avance II 400 or Bruker Avance III 600 NMR spectrometers. NMR spectra are quoted in ppm and were referenced internally relative to the residual protio-solvent (^1H) or solvent (^{13}C) resonances, or externally to $^{15}NH_3$. Where necessary, NMR assignments were confirmed by the use of two-dimensional ^1H–^1H and ^1H–^{13}C correlation experiments. ^{15}N data were obtained by two-dimensional ^1H correlated experiments or by direct detection using a cryogenically cooled direct-detection NMR probe (QNP CryoProbe™). Microanalyses were performed by the analytical services in the chemistry department of the Universität Heidelberg. IR spectra were recorded on a Varian 3100 Exalibur spectrometer as KBr plates. Infrared data are quoted in cm^{-1}.

(A) Preparation of the compounds

[Cp*Ti(N^{Xyl}N)(CH_3)$_2$] (1). [Cp*$TiCl_3$] (1.0 g, 3.5 mmol) was dissolved in toluene (50 ml), and cooled to –40 °C. Methyllithium (1.6 M in diethylether, 6.5 mL, 10.5 mmol) was added dropwise over 30 min. The reaction was stirred for 2 h below –30 °C before a toluene solution of $N^{Xyl}NH$ (658 mg, 3.5 mmol) was added dropwise. The mixture was stirred for additional 2 h under a

Table 5 Intermolecular hydroamination of 1-octyne with primary amines

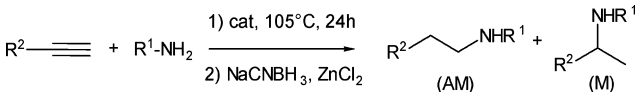

Entry	Alkyne	Amine	Cat.	Isolated yield (%)	Ratio AM : M
1	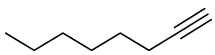	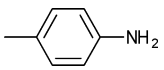	1	87	1 : 7
2			2	93	1 : 14
3			6	96	1 : 10
4	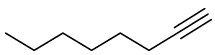	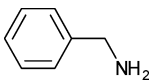	1	57	1 : 7
5			2	54	1 : 9
6	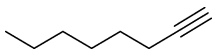	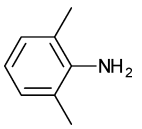	1	91	1 : 99
7			2	92	1 : 99
8			4	92	0 : 100
9	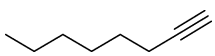	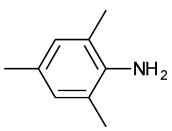	1	88	1 : 99
10			2	87	1 : 99
11			3	88	0 : 1000
12	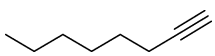	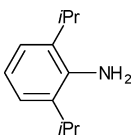	4	42	0 : 100

Reaction conditions: alkyne (2.4 mmol), amine (2.4 mmol), 5 mol% cat. in 1 mL of toluene, 105 °C, 24 h. Reduction: $NaCNBH_3$ (4.8 mmol), $ZnCl_2$ (2.4 mmol), 10 mL methanol, 20 °C, 20 h. Yields determined after column chromatography.

Table 6 Intramolecular hydroaminations

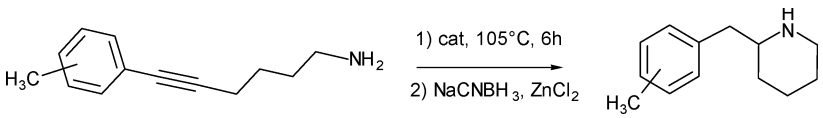

Entry	Aminoalkyne	Cat.	Isolated yield (%)
1	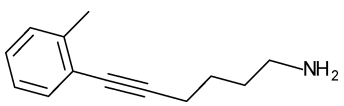	1	98
2		2	95
3	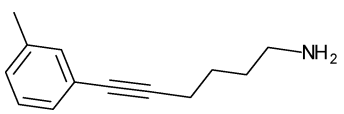	1	97
4		2	97
5	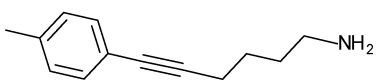	1	98
6		2	96

Reaction conditions: aminoalkyne (2.4 mmol), 5 mol% cat. in 1 mL of toluene, 105 °C, 6 h. Reduction: $NaCNBH_3$ (4.8 mmol), $ZnCl_2$ (2.4 mmol), 10 mL methanol, 20 °C, 20 h. Yields determined after column chromatography.

static vacuum while the solution was allowed to warm to ambient temperature. All volatiles were removed under reduced pressure, the residue suspended in pentane and the supernatant was removed by filtration. From the concentrated pentane solution the desired product crystallized as an orange solid at −80 °C (990 mg, 75% yield). Suitable crystals for X-ray diffraction were grown from a concentrated pentane solution at −18 °C. (Found: C, 71.83, H, 9.05, N, 7.02. Calcd for $C_{24}H_{36}N_2Ti$: C 71.98, H 9.06, N 7.00%). ν_{max} (KBr)/cm^{-1}: 2958 (m), 2945 (m), 2912 (m), 2857 (m), 1618 (m), 1601 (m), 1519 (s), 1472 (m), 793 (s). ^{1}H NMR (399.9 MHz, benzene-d_6, 293 K): δ 6.72 (s, 2 H, *ortho*-$C_6H_3Me_2$), 6.60 (s, 1 H, *para*-$C_6H_3Me_2$), 3.27 (m, 2 H, NCH_2), 2.35 (m, 2 H, $NCCH_2$), 2.20 (s, 6 H, $C_6H_3Me_2$), 1.92 (s, 15 H, C_5Me_5), 1.55 (m, 2 H, NCH_2CH_2), 0.85 (s, 6 H, $TiMe_2$). ^{13}C{^{1}H} NMR (100.6 MHz, benzene-d_6,

293 K): δ 175.0 (N*C*N), 150.3 (*ipso*-$C_6H_3Me_2$), 138.0 (*meta*-$C_6H_3Me_2$), 124.4 (*para*-$C_6H_3Me_2$), 124.5 (C_5Me_5), 122.1 (*ortho*-$C_6H_3Me_2$), 66.6 (Ti*Me*$_2$), 52.2 (N*C*H$_2$), 28.7 (NC*C*H$_2$), 23.9 (NCH$_2$*C*H$_2$), 21.6 (C_6H_3*Me*$_2$), 12.4 (C_5*Me*$_5$).

[Cp*Ti(N^{Xyl}N)(N^{t}Bu)(NH$_2{}^t$Bu)] (2). [Cp*Ti(N^{Xyl}N)(CH$_3$)$_2$] (**1**) (1.6 g, 4 mmol) was dissolved in hexane (20 mL), ^{t}BuNH$_2$ (2.3 mL, 20 mmol) was added and the reaction mixture heated to 70 °C for 24 h. The volatiles were removed under reduced pressure and the crude product was recrystallized from pentane containing 2% ^{t}BuNH$_2$ at −80 °C. The product crystallized as a yellow-orange solid (1.9 g, 95% yield). (Found: C 69.99, H 9.78, N 10.82. Calcd for $C_{30}H_{49}N_4Ti$: C 70.15, H 9.62, N 10.91%). ν_{max} (KBr)/cm^{-1}: 3317 (w), 2959 (s), 2914 (s), 2864 (s), 2833 (m), 1591 (m), 1545 (s), 1454 (m), 1388 (m), 1375 (m), 1265 (m), 1234 (m), 1084 (m). ^{1}H NMR (399.9 MHz, toluene-d$_8$, 218 K): δ 7.28 (d, $^2J_{H-H}$ = 11.1 Hz, 1 H, N*H*$_2{}^t$Bu,), 6.82 (s, 2 H, *ortho*-$C_6H_3Me_2$), 6.65 (s, 1 H, *para*-$C_6H_3Me_2$), 4.21 (m, 1 H, NC*H*$_2$), 3.68 (m, 1 H, NC*H*$_2$), 2.49 (m, 1 H, NCC*H*$_2$), 2.39 (s, 6 H, C_6H_3*Me*$_2$), 2.19 (m, 1 H, NCC*H*$_2$), 2.08 (s, 15 H, C_5*Me*$_5$), 1.80 (d, $^2J_{H-H}$ = 10.9 Hz, 1 H, N*H*$_2{}^t$Bu,), 1.72 (m, 2 H, NCH$_2$C*H*$_2$), 1.40 (s, 9 H, N^{t}Bu), 1.37 (s, 9 H, NH$_2{}^t$Bu). ^{13}C{^{1}H} NMR (100.6 MHz, toluene-d$_8$, 218 K): δ 173.0 (N*C*N), 154.1 (*ipso*-$C_6H_3Me_2$), 138.0 (*meta*-$C_6H_3Me_2$), 122.8 (*para*-$C_6H_3Me_2$), 121.0 (*ortho*-$C_6H_3Me_2$), 116.8 (C_5Me_5), 67.1 (N*C*(CH$_3$)$_3$), 57.5 (N*C*H$_2$), 50.4 (NH$_2$*C*(CH$_3$)$_3$), 33.4 (NC(*C*H$_3$)$_3$), 30.8 (NH$_2$C(*C*H$_3$)$_2$), 29.8 (NC*C*H$_2$), 25.6 (NCH$_2$*C*H$_2$), 22.0 (C_6H_3*Me*$_2$), 12.2 (C_5*Me*$_5$). ^{15}N NMR (60.8 MHz, benzene-d$_6$, 295 K): δ 407.3 (*N*C(CH$_3$)$_3$, 204.6 (Xyl*N*CN), 199.0 (XylNC*N*), 79.4 (*N*H$_2$C(CH$_3$)$_3$).

NMR tube generation of [Cp*Ti(N^{Xyl}N)(N^{t}Bu)] (2a) and [Cp*Ti(N^{Xyl}N)(N^{t}Bu)(Py)] (2b). A solution of [Cp*Ti(N^{Xyl}N)(N^{t}Bu)(NH$_2{}^t$Bu)] (**2**) (36 mg, 0.07 mmol) in benzene-d$_6$ (0.5 mL) was added to B(C$_6$F$_5$)$_3$ (36 mg, 0.07 mmol). The product was added to a Teflon valve NMR tube, sealed, and characterized *in situ.*

[Cp*Ti(N^{Xyl}N)(N^{t}Bu)(Py)] (2a). ^{1}H NMR (399.9 MHz, benzene-d$_6$, 293 K): δ 6.64 (s, 2 H, *ortho*-$C_6H_3Me_2$), 6.58 (s, 1 H, *para*-$C_6H_3Me_2$), 3.51 (m, 2 H, NC*H*$_2$), 2.60 (m, 1 H, NCC*H*$_2$), 2.29 (m, 1 H, NCC*H*$_2$), 2.24 (s, 6 H, C_6H_3*Me*$_2$), 2.00 (s, 15 H, C_5*Me*$_5$), 1.21 (s, 9 H, NC(C*H*$_3$)$_3$), 1.68 (m, 2 H, NCH$_2$C*H*$_2$). ^{13}C{^{1}H} NMR (100.6 MHz, benzene-d$_6$, 293 K): δ 168.1 (N*C*N), 149.2 (*ipso*-$C_6H_3Me_2$), 138.2 (*meta*-$C_6H_3Me_2$), 123.4 (*para*-$C_6H_3Me_2$), 120.3 (*ortho*-$C_6H_3Me_2$), 119.8 (C_5Me_5), 67.3 (N*C*(CH$_3$)), 54.1 (N*C*H$_2$), 33.2 (NC(*C*H$_3$)), 29.4 (NC*C*H$_2$), 24.4 (NCH$_2$*C*H$_2$), 21.6 (C_6H_3*Me*$_2$), 11.8 (C_5*Me*$_5$). Subsequently, few drops of pyridine were added and the solvent was removed after 30 min. The residue was redissolved in benzene-d$_6$ and the NMR spectra of **2b** were recorded.

[Cp*Ti(N^{Xyl}N)(N^{t}Bu)(Py)] (2b). ^{1}H NMR (399.9 MHz, benzene-d$_6$, 293 K): δ 8.49 (d, 2 H, $^3J_{H-H}$ = 4 Hz; *ortho*-C_5H_5N), 6.95 (t, $^3J_{H-H}$ = 7.5 Hz, 1 H, *para*-C_5H_5N), 6.63–6.60 (m, 2 H, *meta*-C_5H_5N, overlapping with *ortho*-$C_6H_3Me_2$), 6.61 (s, 2 H, *ortho*-$C_6H_3Me_2$, overlapping with Py), 6.58 (s, 1 H, *para*-$C_6H_3Me_2$), 3.61 (m, 2 H, NC*H*$_2$), 2.38 (broad m, 2 H, NCH$_2$C*H*$_2$), 2.22 (s, 6 H, C_6H_3*Me*$_2$), 2.07 (s, 15 H, C_5*Me*$_5$), 1.70 (m, 2 H, NCC*H*$_2$), 1.23 (s, 9 H, NC(C*H*$_3$)$_3$). ^{13}C{^{1}H} NMR (100.6 MHz, benzene-d$_6$, 293 K): δ 168.8 (N*C*N), 150.4 (*ortho*-C_5H_5N), 141.8 (*ipso*-$C_6H_3Me_2$), 138.0 (*meta*-$C_6H_3Me_2$), 135.7 (*para*-C_5H_5N), 123.5 (*meta*-C_5H_5N), 123.3 (*para*-$C_6H_3Me_2$), 121.0 (*ortho*-$C_6H_3Me_2$), 118.8 (C_5Me_5), 67.3 (N*C*(CH$_3$)$_3$), 54.9 (N*C*H$_2$), 33.3 (NC(*C*H$_3$)$_3$), 29.4 (NC*C*H$_2$), 24.5 (NCH$_2$*C*H$_2$), 21.6 (C_6H_3*Me*$_2$), 11.9 (C_5*Me*$_5$).

General procedure for the synthesis of imido complexes with aromatic substituents on the imido nitrogen: preparation of [Cp*Ti(N^{Xyl}N)(N-2,4,6-C$_6$H$_2$Me$_3$)] (3), [Cp*Ti(N^{Xyl}N)(N-2,6-C$_6$H$_3$(^{i}Pr)$_2$)] (4) and [Cp*Ti(N^{Xyl}N)(N-2,6-C$_6$H$_3$Me$_2$)] (5). To a solution of [Cp*Ti(N^{Xyl}N)(N^{t}Bu)(NH$_2{}^t$Bu)] (**2**) (1 g, 2 mmol) in hexane (5 mL) was added the appropriate amine (2 mmol), and the solution was stirred at room temperature for 30 min. The imido complexes started to precipitate as green solids, and after stirring for 1 h at room temperature the supernatant was removed by filtration to give the product as a green microcrystalline solid. ([Cp*Ti(N^{Xyl}N)(2,4,6-NC$_6$H$_2$Me$_3$)] (**3**): 734 mg, 75% yield, [Cp*Ti(N^{Xyl}N)(2,6-NC$_6$H$_3$(^{i}Pr)$_2$)] (**4**): 819 mg, 71% yield, [Cp*Ti(N^{Xyl}N)(2,6-NC$_6$H$_3$Me$_2$)] (**5**): 685 mg, 68% yield).

[Cp*Ti(N^{Xyl}N)(N-2,4,6-C$_6$H$_2$Me$_3$)] (3). Suitable crystals for X-ray analysis were obtained from a concentrated hexane solution at −18 °C. (Found: C 73.77, H 8.22, N 8.32. Calcd for $C_{31}H_{41}N_3Ti$: C 73.94, H 8.21, N 8.34%). ν_{max} (KBr)/cm^{-1}: 2910 (m), 2854 (m), 1593 (s), 1502 (s), 1465 (s), 1309 (s), 1286 (s), 782 (s). ^{1}H NMR (399.9 MHz, benzene-d$_6$, 295 K): δ 6.82 (s, 2 H, *meta*-$C_6H_2Me_3$), 6.66 (s, 2 H, *ortho*-$C_6H_3Me_2$), 6.60 (s, 1 H, *para*-$C_6H_3Me_2$), 3.48 (m, 2 H, NC*H*$_2$), 2.47 (m, 1 H, NCC*H*$_2$), 2.38 (s, 6 H, *ortho*-C_6H_2*Me*$_3$), 2.25 (s, 6 H, C_6H_3*Me*$_2$), 2.22 (s, 3 H, *para*-C_6H_2*Me*$_3$), 2.17 (m, 1 H, NCC*H*$_2$), 1.99 (s, 15 H, C_5*Me*$_5$), 1.51 (m, 2 H, NCH$_2$C*H*$_2$). ^{13}C{^{1}H} NMR (100.6 MHz, benzene-d$_6$, 295 K): δ 167.8 (N*C*N), 156.7 (*ipso*-$C_6H_2Me_3$), 148.4 (*ipso*-$C_6H_3Me_2$), 138.4 (*meta*-$C_6H_3Me_2$), 131.4 (*ortho*-$C_6H_2Me_3$), 128.5 (*meta*-$C_6H_2Me_3$), 128.2 (*para*-$C_6H_2Me_3$), 123.6 (*para*-$C_6H_3Me_2$), 121.1 (C_5Me_5), 120.2 (*ortho*-$C_6H_3Me_2$), 53.5 (N*C*H$_2$), 29.8 (NC*C*H$_2$), 24.3 (NCH$_2$*C*H$_2$), 21.6 (C_6H_3*Me*$_2$), 21.2 (*para*-C_6H_2*Me*$_3$), 19.9 (*ortho*-C_6H_2*Me*$_3$), 11.5 (C_5*Me*$_5$).

[Cp*Ti(N^{Xyl}N)(N-2,6-C$_6$H$_3$(^{i}Pr)$_2$)] (4). Suitable crystals for X-ray diffraction were obtained from a concentrated hexane solution at 10 °C. (Found: C 74.82, H 8.67, N 7.62. Calcd for $C_{34}H_{47}N_3Ti$: C 74.84, H 8.68, N 7.70%). ν_{max} (KBr)/cm^{-1}: 3039 (w), 2960 (m), 2913 (m), 1619 (m), 1501 (m), 1459 (m), 1438 (m), 1355 (m), 784 (s). ^{1}H NMR (399.9 MHz, benzene-d$_6$, 295 K): δ 7.05 (d, $^3J_{H-H}$ = 7.6 Hz, 2 H, *meta*-$C_6H_3(^iPr)_2$), 6.88 (t, $^3J_{H-H}$ = 7.6 Hz, 1 H, *para*-$C_6H_3(^iPr)_2$), 6.59 (overlapping s, 3 H, *ortho*-$C_6H_3Me_2$, *para*-$C_6H_3Me_2$), 3.64 (septet, $^3J_{H-H}$ = 6.9 Hz, 2 H, $C_6H_3(CH(CH_3)_2)_2$), 3.54 (m, 1 H, NC*H*$_2$), 3.40 (m, 1 H, NC*H*$_2$), 2.49 (m, 1 H, NCC*H*$_2$), 2.26 (m, 1 H, NCC*H*$_2$), 2.27 (s, 6 H, C_6H_3*Me*$_2$), 1.98 (s, 15 H, C_5*Me*$_5$), 1.56 (m, 2 H, NCH$_2$C*H*$_2$), 1.37 (d, $^3J_{H-H}$ = 6.4 Hz, 6 H, $C_6H_3(CH(CH_3)_2)_2$), 1.32 (d, $^3J_{H-H}$ = 7.2 Hz, 6 H, $C_6H_3(CH(CH_3)_2)_2$). ^{13}C{^{1}H} NMR (100.6 MHz, benzene-d$_6$, 295 K): δ 167.0 (N*C*N), 155.2 (*ipso*-$C_6H_3(^iPr)_2$), 147.9 (*ipso*-$C_6H_3Me_2$), 143.3 (*ortho*-$C_6H_3(^iPr)_2$), 138.4 (*meta*-$C_6H_3Me_2$), 123.4 (*ortho*- or *para*-$C_6H_3Me_2$), 122.3 (*meta*-$C_6H_3(^iPr)_2$), 121.4 (C_5Me_5), 120.3 (*para*-$C_6H_3(^iPr)_2$), 119.6 (*ortho*- or *para*-$C_6H_3Me_2$), 52.3 (N*C*H$_2$), 30.2 (NC*C*H$_2$), 28.4 ($C_6H_3(CH(CH_3)_2)_2$), 24.6 (NCH$_2$*C*H$_2$), 24.4 ($C_6H_3(CH(CH_3)_2)_2$), 24.2 ($C_6H_3(CH(CH_3)_2)_2$), 21.7 (C_6H_3*Me*$_2$), 11.5 (C_5*Me*$_5$).

[Cp*Ti(N^{Xyl}N)(N-2,6-C$_6$H$_3$Me$_2$)] (5). Suitable crystals for X-ray diffraction were obtained from a concentrated hexane solution at −18 °C. (Found: C 73.60, H 8.02, N 8.70. Calcd for $C_{30}H_{39}N_3Ti$: C 73.60, H 8.03, N 8.58%). ν_{max} (KBr)/cm^{-1}: 3024 (w), 2950

(m), 2910 (m), 2853 (m), 1596 (s), 1492 (s), 1457 (s), 1291 (s), 1196 (m). ^{1}H NMR (600.1 MHz, benzene-d$_6$, 295 K): δ 7.03 (d, $^3J_{H-H}$ = 7.6 Hz, 2 H, *meta*-2,6-C$_6H_3$Me$_2$), 6.74 (t, $^3J_{H-H}$ = 7.1 Hz, 1 H, *para*-2,6-C$_6H_3$Me$_2$), 6.65 (s, 2 H, *ortho*-3,5-C$_6H_3$Me$_2$), 6.60 (s, 1 H, *para*-3,5-C$_6H_3$Me$_2$), 3.45 (m, 2 H, NCH_2), 2.47 (m, 1 H, NCCH_2), 2.37 (s, 6 H, 2,6-C$_6$H$_3$*Me*$_2$), 2.24 (s, 6 H, 3,5-C$_6$H$_3$*Me*$_2$), 2.16 (m, 1 H, NCCH_2), 1.98 (s, 15 H, C$_5$*Me*$_5$), 1.52 (m, 2 H, NCH$_2$CH_2). ^{13}C{^{1}H} NMR (150.1 MHz, benzene-d$_6$, 293 K): δ 167.9 (N*C*N), 158.6 (*ipso*-2,6-*C*$_6$H$_3$Me$_2$), 148.1 (*ipso*-3,5-*C*$_6$H$_3$Me$_2$), 138.3 (*meta*-3,5-*C*$_6$H$_3$Me$_2$), 131.5 (*ortho*-2,6-*C*$_6$H$_3$Me$_2$), 127.6 (*meta*-2,6-*C*$_6$H$_3$Me$_2$), 123.7 (*para*-3,5-*C*$_6$H$_3$Me$_2$), 121.2 (*C*$_5$Me$_5$), 120.1 (*ortho*-3,5-*C*$_6$H$_3$Me$_2$), 119.2 (*para*-2,6-*C*$_6$H$_3$Me$_2$), 53.4 (N*C*H$_2$), 29.6 (NC*C*H$_2$), 24.2 (NCH$_2$*C*H$_2$), 21.4 (3,5-C$_6$H$_3$*Me*$_2$), 19.8 (2,6-C$_6$H$_3$*Me*$_2$), 11.4 (C$_5$*Me*$_5$).

NMR tube generation of [Cp*Ti(N^{Xyl}N)(N-4-C$_6$H$_4$Me)-(NH$_2$^{t}Bu)] (6a). In the glove box [Cp*Ti(N^{Xyl}N)(N^{t}Bu)-(NH$_2$^{t}Bu)] (**2**) (24 mg, 0.05 mmol) was dissolved in benzene-d$_6$ (0.5 mL), *p*-toluidine (5 mg, 0.05 mmol) was added and the NMR spectra were recorded. ^{1}H NMR (399.9 MHz, benzene-d$_6$, 293 K): δ 7.00 (d, $^3J_{H-H}$ = 8.0 Hz, 2 H, *ortho*- or *meta*-C$_6H_4$Me), 6.89 (d, $^3J_{H-H}$ = 7.9 Hz, 2 H, *ortho*- or *meta*-C$_6H_4$Me), 6.69 (s, 2 H, *ortho*-C$_6H_3$Me$_2$), 6.63 (s, 1 H, *para*-C$_6H_3$Me$_2$), 4.18 (m, 1 H, NCH_2), 3.66 (m, 1 H, NCH_2), 2.38 (m, 1 H, NCCH_2), 2.28 (s, 6 H, C$_6$H$_3$*Me*$_2$), 2.21 (s, 3 H, *para*-C$_6$H$_4$*Me*), 2.05 (m, 1 H, NCCH_2), 1.97 (s, 15 H, C$_5$*Me*$_5$), 1.61 (m, 2 H, NCH$_2$CH_2), 1.25 (s, 9 H, NH$_2$C(CH_3)$_3$), NH_2C(CH$_3$) not observed. ^{13}C{^{1}H} NMR (100.6 MHz, benzene-d$_6$, 293 K): δ 173.4 (N*C*N), 153.6 (broad *ispo*-*C*$_6$H$_3$Me$_2$), 138.3 (*meta*-*C*$_6$H$_3$Me$_2$), 129.4 (*ortho*- or *meta*-*C*$_6$H$_4$Me$_2$), 123.8 (broad *para*-*C*$_6$H$_3$Me$_2$ and *ortho*- or *meta*-*C*$_6$H$_4$Me), 121.0 (*ortho*-*C*$_6$H$_3$Me$_2$), 118.8 (*C*$_5$Me$_5$), 51.2 (broad H$_2$N*C*(CH$_3$)$_3$), 48.0 (broad N*C*H$_2$), 32.2 (NH$_2$C(*C*H$_3$)$_3$), 29.8 (NC*C*H$_2$); 23.0 (NCH$_2$*C*H$_2$); 21.8 (C$_6$H$_3$*Me*$_2$); 20.9 (C$_6$H$_4$*Me*); 11.6 (C$_5$*Me*$_5$), *ipso*-*C*$_6$H$_4$Me not observed.

[Cp*Ti(N^{Xyl}N)(N-4-C$_6$H$_4$Me)(NC$_5$H$_5$)] (6). To a solution of [Cp*Ti(N^{Xyl}N)(N^{t}Bu)(NH$_2$^{t}Bu)] (**2**) (564 mg, 1.1 mmol) in toluene was added a solution of *p*-toluidine (110 mg, 1.1 mmol) in toluene dropwise. The dark red solution was stirred for 1 h before pyridine (0.2 ml, 2.2 mmol) was added. The reaction mixture was stirred an additional hour at room temperature before all volatiles were removed under reduced pressure. The residue was washed with pentane and the product was obtained as orange powder (305 mg, 50% yield). Found C 73.21, H 7.64, N 9.91. Calcd for C$_{34}$H$_{42}$N$_4$Ti: C 73.63, H 7.63, N 10.10%. ν_{max} (KBr)/cm^{-1}: 2964 (m), 2911 (m), 1858 (m), 1620 (s), 1598 (s), 1536 (s), 1485 (s), 1309 (s), 1288 (s). ^{1}H NMR (399.9 MHz, benzene-d$_6$, 295 K): δ 8.74 (d, $^3J_{H-H}$ = 5.1 Hz, 2 H, *ortho*-C$_5H_5$N,), 7.05–7.00 (m, 4 H, *ortho*- and *meta*-C$_6H_4$Me), 6.85 (s, 2 H, *ortho*-C$_6H_3$Me$_2$), 6.81 (m, 1 H, *para*-C$_5H_5$N), 6.60 (s, 1 H, *para*-C$_6H_3$Me$_2$), 6.53 (m, 2 H, *meta*-C$_5H_5$N), 3.40 (broad m, 2 H, NCH_2), 2.22 (s, 3 H, C$_6$H$_4$*Me*), 2.21 (s, 6 H, C$_6$H$_3$*Me*$_2$), 1.99 (s, 15 H, C$_5$*Me*$_5$), 1.50 (m, 2 H, NCH$_2$CH_2). ^{13}C{^{1}H} NMR (100.6 MHz, benzene-d$_6$, 295 K): δ 172.7 (N*C*N), 158.5 (*ipso*-*C*$_6$H$_4$Me), 152.5 (*ortho*-*C*$_5$H$_5$N), 151.3 (*ipso*-*C*$_6$H$_3$Me$_2$), 137.6 (*meta*-*C*$_6$H$_3$Me$_2$), 136.6 (*para*-*C*$_5$H$_5$N), 129.1 (*ortho*- or *meta*-*C*$_6$H$_4$Me), 123.8 (*ortho*- or *meta*-*C*$_6$H$_4$Me), 123.5 (*para*-*C*$_6$H$_3$Me$_2$), 123.4 (*meta*-*C*$_5$H$_5$N), 123.1 (*ortho*-*C*$_6$H$_3$Me$_2$), 118.2 (*C*$_5$Me$_5$), 54.2 (N*C*H$_2$), 29.3 (NC*C*H$_2$), 23.5 (NCH$_2$*C*H$_2$), 21.6 (C$_6$H$_4$*Me*$_2$), 21.6 (C$_6$H$_3$*Me*$_2$), 12.0 (C$_5$*Me*$_5$), not observed: *para*-*C*$_6$H$_4$Me.

General preparative procedure for the synthesis of acetylido-amido complexes [Cp*Ti(N^{Xyl}N)(CCPh)(NH^{t}Bu)] (7) and [Cp*Ti(N^{Xyl}N)(CCTol)(NH^{t}Bu)] (8). To a solution of [Cp*Ti-(N^{Xyl}N)(N^{t}Bu)(NH^{t}Bu)] (**2**) (327 mg, 0.637 mmol) in toluene (20 mL) was added the appropriate acetylene (70 μL, 0.637 mmol), producing an immediate colour change to bright orange. After stirring for 1 h at room temperature the solvent was removed and the product recrystallized as a bright yellow solid from pentane at −80 °C. ([Cp*Ti(N^{Xyl}N)(CCPh)(NH^{t}Bu)] (**7**) 219 mg, 63% yield, [Cp*Ti(N^{Xyl}N)(CC-p-Tol)(NH^{t}Bu)] (**8**) 217 mg, 58% yield).

[Cp*Ti(N^{Xyl}N)(CCPh)(NH^{t}Bu)] (7). (Found: C 74.88, H 8.33, N 7.85. Calcd for C$_{34}$H$_{45}$N$_3$Ti: C 75.12, H 8.34, N 7.73%). ν_{max} (KBr)/cm^{-1}: 3332 (w), 3284 (w), 2948 (m), 2910 (m), 1860 (m), 1594 (s), 1558 (s), 1459 (s), 1374 (s), 1287 (s), 1095 (m). ^{1}H NMR (399.9 MHz, benzene-d$_6$, 295 K): δ 8.46 (s, 1 H, NH^tBu), 7.59 (d, $^3J_{H-H}$ = 7.1 Hz, 2 H, *ortho*-C$_6H_5$), 7.13 (m, 2 H, *meta*-C$_6H_5$), 7.00 (t, $^3J_{H-H}$ = 7.4 Hz, 1 H, *para*-C$_6H_5$), 6.74 (s, 2 H, *ortho*-C$_6H_3$Me$_2$), 6.56 (s, 1 H, *para*-C$_6H_3$Me$_2$), 4.24 (m, 1 H, NCH_2), 3.57 (m, 1 H, NCH_2), 2.49 (m, 1 H, NCCH_2), 2.27 (s, 6 H, C$_6$H$_3$*Me*$_2$), 2.13 (m, 1 H, NCCH_2), 2.08 (s, 15 H, C$_5$*Me*$_5$), 1.60 (m, 2 H, NCH$_2$CH_2), 1.39 (s, 9 H, NHC(CH_3)$_3$). ^{13}C{^{1}H} NMR (100.6 MHz, benzene-d$_6$, 295 K): δ 173.1 (N*C*N), 153.2 (*C*CPh), 147.9 (*ipso*-*C*$_6$H$_3$Me$_2$), 137.7 (*meta*-*C*$_6$H$_3$Me$_2$), 131.0 (*ortho*-*C*$_6$H$_5$), 128.4 (*meta*-*C*$_6$H$_5$), 125.6 (*para*-*C*$_6$H$_5$), 122.8 (*C*$_5$Me$_5$), 122.6 (*para*-*C*$_6$H$_3$Me$_2$), 120.2 (*ortho*-*C*$_6$H$_3$Me$_2$), 108.8 (C*C*Ph), 60.3 (NH*C*(CH$_3$)$_3$), 53.3 (N*C*H$_2$), 31.2 (NHC(*C*H$_3$)$_3$), 30.2 (NC*C*H$_2$), 24.5 (NCH$_2$*C*H$_2$), 21.6 (C$_6$H$_3$*Me*$_2$), 13.2 (C$_5$*Me*$_5$). ^{15}N NMR (60.8 MHz, benzene-d$_6$, 295 K): δ 331.1 (*N*H^{t}Bu, $^1J_{N-H}$ = 62.6 Hz), 216.2 (*N*CNXyl), 174.5 (NC*N*Xyl).

[Cp*Ti(N^{Xyl}N)(CC-p-Tol)(NH^{t}Bu)] (8). (Found: C 72.06, H 8.31, N 7.13. Calcd for C$_{35}$H$_{47}$N$_3$Ti: C 75.38, H 8.49, N 7.53%, value for carbon is too low owing to incomplete combustion). ν_{max} (KBr)/cm^{-1}: 3429 (w), 2956 (m), 2910 (m), 2859 (m), 1592 (m), 1504 (s), 1512 (s), 1467 (m), 1289 (s), 1201 (m), 1185 (m), 1097 (m). ^{1}H NMR (399.9 MHz, benzene-d$_6$, 295 K): δ 8.46 (s, 1 H, NH^tBu), 7.56 (d, $^3J_{H-H}$ = 7.5 Hz, 2 H, *ortho*-C$_6H_4$Me), 6.99 (d, $^3J_{H-H}$ = 7.9 Hz, 2 H, *meta*-C$_6H_4$Me), 6.75 (s, 2 H, *ortho*-C$_6H_3$Me$_2$), 6.56 (s, 1 H, *para*-C$_6H_3$Me$_2$), 4.29 (m, 1 H, NCH_2), 3.59 (m, 1 H, NCH_2), 2.47 (m, 1 H, NCCH_2), 2.27 (s, 6 H, C$_6$H$_3$*Me*$_2$), 2.11 (m, 1 H, NCCH_2), 2.09 (s, 15 H, C$_5$*Me*$_5$), 2.08 (s, 3 H, C$_6$H$_4$*Me*), 1.60 (m, 2 H, NCH$_2$CH_2). ^{13}C{^{1}H} NMR (100.6 MHz, benzene-d$_6$, 295 K): δ 173.1 (N*C*N), 152.5 (*C*C-Tol), 148.0 (*ipso*-*C*$_6$H$_3$Me$_2$), 137.7 (*meta*-*C*$_6$H$_3$Me$_2$), 135.1 (*ipso*-*C*$_6$H$_4$Me), 131.0 (*ortho*-*C*$_6$H$_4$Me), 129.2 (*meta*-*C*$_6$H$_4$Me), 125.5 (*para*-*C*$_6$H$_4$Me), 122.8 (*C*$_5$Me$_5$), 122.5 (*ortho*-*C*$_6$H$_3$Me$_2$), 120.1 (*para*-*C*$_6$H$_3$Me$_2$), 108.6 (C*C*-Tol), 60.4 (NH*C*(CH$_3$)$_3$), 53.3 (N*C*H$_2$), 31.2 (NHC(*C*H$_3$)$_3$), 30.2 (NC*C*H$_2$), 24.5 (NCH$_2$*C*H$_2$), 21.7 (C$_6$H$_3$*Me*$_2$), 21.3 (C$_6$H$_4$*Me*), 13.1 (C$_5$*Me*$_5$). ^{15}N NMR (60.8 MHz, benzene-d$_6$, 295 K): δ 331.1 (*N*H^{t}Bu, $^1J_{N-H}$ = 62.6 Hz), 216.2 (*N*CNXyl), 174.5 (NC*N*Xyl).

General procedure for the synthesis of azatitanacycles Cp*Ti(N^{Xyl}N){κ^{2}N(2,4,6-C$_6$H$_2$Me$_3$)CPh=CH}] (9), [Cp*Ti-(N^{Xyl}N){κ^{2}N(2,6-C$_6$H$_3$Me$_2$)CPh=CH}] (10), and Cp*Ti(N^{Xyl}N)-{κ^{2}N(2,6-C$_6$H$_3$Me$_2$)CTol=CH}] (11). To a stirred solution of the appropriate imido complex (1.3 mmol) in toluene (10 mL) was added the appropriate acetylene (2.6 mmol) dropwise. The solution immediately turned dark brown. After 4 h all volatiles were removed under reduced pressure and the crude product was dissolved in pentane whilst

maintaining the temperature below 0 °C. The product crystallized at −30 °C as a deep brown microcrystalline solid. ([Cp*Ti(N^{Xyl}N){κ^{2}N(2,4,6-$C_6H_2Me_3$)CPh=CH}] (**9**): 377 mg, 48% yield, ([Cp*Ti(N^{Xyl}N){κ^{2}N(2,6-$C_6H_3Me_2$)CPh=CH}] (**10**): 472 mg, 74% yield, [Cp*Ti(N^{Xyl}N){κ^{2}N(2,6-$C_6H_3Me_2$)CTol=CH}] (**11**): 471 mg, 60% yield).

[Cp*Ti(N^{Xyl}N){κ^{2}N(2,4,6-$C_6H_2Me_3$)CPh=CH}] (9). (Found: C 76.94, H 7.81, N 6.58. Calcd for $C_{39}H_{47}N_3Ti$: C 77.33, H 7.82, N 6.94%). ν_{max} (KBr)/cm^{-1}: 2943 (w), 2009 (m), 2855 (m), 1637 (m), 1592 (s), 1534 (s), 1482 (s), 1433 (s), 1308 (m), 1274 (m), 788 (s). ^{1}H NMR (399.9 MHz, benzene-d$_6$, 295 K): δ 11.10 (s, 1 H, C=C*H*), 7.46 (m, 2 H, *ortho*-C_6H_5), 7.03 (m, 2 H, *meta*-C_6H_5), 6.93 (s, 1 H, *meta*-$C_6H_2Me_3$), 6.90 (m, 1 H, *para*-C_6H_5), 6.55 (s, 3 H, overlapping *ortho*- and *para*-$C_6H_3Me_2$), 6.44 (s, 1 H, *meta*-$C_6H_2Me_3$), 3.57 (m, 1 H, NCH_2), 3.05 (m, 1 H, NCH_2), 2.48 (m, 1 H, NCCH_2), 2.56 (s, 3 H, *para*-$C_6H_2Me_3$), 2.24 (s, 6 H, $C_6H_3Me_2$), 2.10 (s, 3 H, *ortho*-$C_6H_2Me_3$), 2.08 (s, 3 H, *ortho*-$C_6H_2Me_3$), 1.99 (m, 1 H, NCCH_2), 1.90 (s, 15 H, C_5Me_5), 1.46 (m, 1 H, NCH$_2$CH_2), 1.02 (m, 1 H, NCH$_2$CH_2). ^{13}C{^{1}H} NMR (100.6 MHz, benzene-d$_6$, 295 K): δ 228.4 (C=*C*H), 173.7 (N*C*N), 149.0 (*ipso*-$C_6H_2Me_3$), 148.7 (*ipso*-$C_6H_3Me_2$), 147.3 (*C*=CH), 137.7 (*meta*-$C_6H_3Me_2$), 137.4 (*ipso*-C_6H_5), 131.8 (*para*-$C_6H_2Me_3$), 131.1 (*ortho*-$C_6H_2Me_3$), 129.7 (*meta*-$C_6H_2Me_3$), 128.6 (*meta*-$C_6H_2Me_3$), 127.9 (*para*-C_6H_5), 127.5 (*meta*-C_6H_5), 126.9 (*ortho*-C_6H_5), 123.8 (*ortho*- or *para*-$C_6H_3Me_2$), 122.6 (C_5Me_5), 120.5 (*ortho*- or *para*-$C_6H_3Me_2$), 53.2 (N*C*H$_2$), 30.4 (NC*C*H$_2$), 23.9 (NCH$_2$*C*H$_2$), 21.7 ($C_6H_3Me_2$), 20.8 (*ortho*-$C_6H_2Me_3$), 20.5 (*para*-$C_6H_2Me_3$), 19.8 (*ortho*-$C_6H_2Me_3$), 12.0 (C_5Me_5). Second *ortho*-$C_6H_2Me_3$ not observed.

[Cp*Ti(N^{Xyl}N){κ^{2}N(2,6-$C_6H_3Me_2$)CPh=CH}] (10). (Found: C 76.76, H 7.67, N 7.00. Calcd for $C_{38}H_{45}N_3Ti$: C 77.14, H 7.67, N 7.10%). ν_{max} (KBr)/cm^{-1}: 3020 (w), 2960 (m), 2912 (m), 2856 (m), 1636 (m), 1591 (s), 1503 (s), 1485 (s), 1293 (s), 1090 (m), 784 (s). ^{1}H NMR (600.1 MHz, toluene-d$_8$, 258 K): δ 11.08 (s, 1 H, C=C*H*), 7.44 (d, $^3J_{H-H}$ = 8.0 Hz, 2 H, *ortho*-C_6H_5), 7.10 (d, $^3J_{H-H}$ = 7.8 Hz, 1 H, *meta*-2,6-$C_6H_3Me_2$), 7.04–6.99 (m, *meta*-C_6H_5, overlapping with toluene-d$_8$ signal), 6.89 (t, $^3J_{H-H}$ = 7.2 Hz, 1 H, *para*-C_6H_5), 6.76 (t, $^3J_{H-H}$ = 7.2 Hz, 1 H, *para*-2,6-$C_6H_3Me_2$,), 6.61 (d, $^3J_{H-H}$ = 7.7 Hz, 1 H, *meta*-2,6-$C_6H_3Me_2$), 6.52 (s, 1 H, *para*-3,5-$C_6H_3Me_2$), 6.50 (s, 2 H, *ortho*-3,5-$C_6H_3Me_2$), 3.51 (m, 1 H, NCH_2), 3.00 (m, 1 H, NCH_2), 2.57 (s, 3 H, *ortho*-2,6-$C_6H_3Me_2$), 2.36 (m, 1 H, NCCH_2), 2.26 (s, 6 H, *meta*-3,5-$C_6H_3Me_2$), 2.05 (s, 3 H, *ortho*-2,6-$C_6H_3Me_2$), 1.90 (m, 1 H, NCCH_2), 1.88 (s, 15 H, C_5Me_5), 1.43 (m, 1 H, NCH$_2$CH_2), 0.84 (m, 1 H, NCH$_2$CH_2). ^{13}C{^{1}H} NMR (150.9 MHz, toluene-d$_8$, 258 K): δ 228.2 (C=*C*H), 174.1 (N*C*N), 152.0 (*ipso*-2,6-$C_6H_3Me_2$), 148.9 (*ipso-3,5*-$C_6H_3Me_2$), 147.2 (*C*=CH), 138.1 (*meta-3,5*-$C_6H_3Me_2$), 137.6 (*ipso*-C_6H_5), 132.4 (*ortho-2,6*-$C_6H_3Me_2$), 130.9 (*ortho*-2,6-$C_6H_3Me_2$), 129.5 (*meta*-2,6-$C_6H_3Me_2$), 128.8 (*meta*-C_6H_5), 128.5 (*para*-C_6H_5), 128.3 (*meta*-2,6-$C_6H_3Me_2$), 127.2 (*ortho*-C_6H_5), 124.7 (*para*-3,5-$C_6H_3Me_2$), 123.0 (C_5Me_5), 122.8 (*para*-2,6-$C_6H_3Me_2$), 120.7 (*ortho*-3,5-$C_6H_3Me_2$), 53.7 (N*C*H$_2$), 30.81 (NC*C*H$_2$), 24.4 (NCH$_2$*C*H$_2$), 22.3 (3,5-$C_6H_3Me_2$), 21.2 (2,6-$C_6H_3Me_2$), 20.5 (2,6-$C_6H_3Me_2$), 12.5 (C_5Me_5).

[Cp*Ti(N^{Xyl}N){κ^{2}N(2,6-$C_6H_3Me_2$)CTol=CH}] (11). Suitable crystals for X-ray diffraction were obtained from a concentrated pentane solution at −30 °C. (Found: C 76.77, H 8.19, N 6.46. Calcd for $C_{39}H_{47}N_3Ti$: C 77.33, H 7.82, N 6.94%). ν_{max} (KBr)/cm^{-1}: 3024 (w), 2954 (m), 2914 (s), 2856 (m), 1638 (m), 1590 (s), 1503 (s), 1467 (s), 1375 (m), 1292 (s), 1181 (m), 1090 (m), 785 (s). ^{1}H NMR (600.1 MHz, toluene-d$_8$, 263 K): δ 11.14 (s, 1 H, C=C*H*), 7.12 (s, 1 H, *meta*-2,6-$C_6H_3Me_2$, overlapping with toluene-d$_8$) 7.36 (d, $^3J_{H-H}$ = 8.1 Hz, 2 H, *ortho*-C_6H_4Me), 6,86–6.77 (m, 2 H, *meta*-C_6H_4Me and m, 1 H, *para*-2,6-$C_6H_3Me_2$), 6.65 (d, $^3J_{H-H}$ = 7.9 Hz, 1 H, *meta*-2,6-$C_6H_3Me_2$), 6.52 (s, 3 H, *ortho*- and *para*-3,5-$C_6H_3Me_2$), 3.53 (m, 1 H, NCH_2), 3.05–3.01 (m, 1 H, NCH_2), 2.59 (s, 3 H, 2,6-$C_6H_3Me_2$) 2.41–2.36 (m, 1 H, NCCH_2), 2.26 (s, 6 H, 3,5-$C_6H_3Me_2$), 2.10 (2,6-$C_6H_3Me_2$ overlapping with toluene-d$_8$), 1.94–1.91 (m, 1 H, NCCH_2, overlapping with C_6H_4Me and C_5Me_5), 1.94 (s, 3 H, C_6H_4Me), 1.91 (s, 15 H, C_5Me_5), 1.44 (m, 1 H, NCH$_2$CH_2), 1.25 (m, 1 H, NCH$_2$CH_2). ^{13}C{^{1}H} NMR (150.9 MHz, toluene-d$_8$, 263 K): δ 228.9 (C=*C*H), 174.1 (N*C*N), 152.2 (*ipso*-2,6-$C_6H_3Me_2$), 148.9 (*ipso*-3,5-$C_6H_3Me_2$), 147.5 (*C*=CH), 138.1 (*meta*-3,5-$C_6H_3Me_2$), 134.7 (*ispo*-C_6H_4Me), 132.4 (*ortho-2,6*-$C_6H_3Me_2$), 131.0 (*para*-C_6H_4Me), 129.7 (*meta*-C_6H_4Me), 129.6 (*meta-2,6*-$C_6H_3Me_2$), 128.7 (*meta*-2,6-$C_6H_3Me_2$), 127.2 (*ortho*-C_6H_4Me), 124.2 (*ortho*- or *para*-3,5-$C_6H_3Me_2$), 122.7 (*para*-2,6-$C_6H_3Me_2$), 122.5 (C_5Me_5), 120.8 (*ortho*- or *para*-3,5-$C_6H_3Me_2$), 53.8 (N*C*H$_2$), 35.0 (NC*C*H$_2$), 30.9 (NCH$_2$*C*H$_2$), 22.2 (*meta*-3,5-$C_6H_3Me_2$), 21.6 (*para*-C_6H_4Me), 20.5 (*ortho*-2,6- $C_6H_3Me_2$), 12.5 (C_5Me_5). Second *ortho*-2,6-$C_6H_3Me_2$ not observed.

(B) Kinetic Studies of the {2 + 2}-cycloaddition of phenylacetylene to the imido complex 5, the cycloreversion reaction of the metallacycle 10 to the imido compound 5 and phenylacetylene and the aminolysis of the azatitanacyle 10 with 2,6-dimethylaniline

A solution of [Cp*Ti(N^{Xyl}N)(N-2,6-$C_6H_3Me_2$)] (**5**) (9.8 mg, 20 μmol) and 1,4-dimethoxybenzene (3 mg, internal standard) in toluene-d$_8$ was transferred into a J. Young NMR tube. After cooling the solution to 10 °C, 0.5–5 equiv. of phenylacetylene (10–100 μmol) were added. The tube was transferred to a NMR spectrometer probe that had been pre-cooled to 10 °C. ^{1}H NMR spectra were recorded every 3 min for a period of up to 30 min. The concentration of the reaction product was plotted against time, and the conversion curve was line-fitted to a first order exponential decay A$\exp(-x/b)$. The initial rate was estimated from −A/b, derived from differentiation of the fitted line for $x = 0$. A plot of the initial rate *versus* alkyne concentration indicated a linear relationship.

A solution of [Cp*Ti(N^{Xyl}N)(N-2,6-$C_6H_3Me_2$)] (**5**) (5–25 μmol) and 1,4-dimethoxybenzene (3 mg, internal standard) in toluene-d$_8$ was transferred into a J. Young NMR tube. After cooling the solution to 0 °C, 20 equiv. of phenylacetylene (0.1–0.5 mmol) were added. The tube was transferred to a NMR spectrometer probe that had been pre-cooled to 0 °C. ^{1}H NMR spectra were recorded every 3 min for a period of up to 30 min. The concentration of the reaction product was plotted against time, and the conversion curve was line-fitted to a first order exponential decay A$\exp(-x/b)$. The initial rate was estimated from −A/b, derived from differentiation of the fitted line for $x = 0$. A plot of the initial rate *versus* titanium concentration indicated a linear relationship.

A solution of [Cp*Ti(N^{Xyl}N)(N-2,6-$C_6H_3Me_2$)] (**5**) (20 μmol) in toluene-d$_8$ (0.5 mL) was transferred into a J. Young NMR tube. After cooling the solution to 0 °C, 5 °C, 7.5 °C or 10 °C a solution

of phenylacetylene (20 μmol) in toluene-d_8 (0.1 mL) was added. The tube was transferred to a NMR spectrometer probe that had been pre-cooled. ^{1}H NMR spectra were recorded every 3 min for a period of up to 60 min and then every 10 min for a period of up to 50 min. $(1/[I]) - (1/[I_0])$ was plotted against the time (sec). The second order rate coefficient k_1 was obtained from the slope of the graph. For the Arrhenius plot the rate coefficients were plotted against $1/T$ to yield a straight line. The rate coefficient for 20 °C was estimated graphically as 1.13×10^{-2} L mol^{-1} s^{-1}.

A solution of [Cp*Ti(N^{Xyl}N){κ^{2}N(2,6-$C_6H_3Me_2$)CPh=CH}] (**10**) (5–25 μmol) and 1,4-dimethoxybenzene (3 mg, internal standard) in benzene-d_6 was transferred into a J. Young NMR tube. The tube was transferred to a NMR spectrometer probe that had been pre-cooled to 20 °C. ^{1}H NMR spectra were recorded every 5–10 min for a period of up to 50–100 min. The concentration of [Cp*Ti(N^{Xyl}N){κ^{2}N(2,6-$C_6H_3Me_2$)CPh=CH}] (**10**) was plotted against time, and the conversion curve was line-fitted to a first order exponential decay Aexp(−x/b). The initial rate was estimated from −A/b, derived from differentiation of the fitted line for $x = 0$. A plot of the initial rate *versus* the concentration of [Cp*Ti(N^{Xyl}N){κ^{2}N(2,6-$C_6H_3Me_2$)CPh=CH}] (**10**) indicated a linear relationship, from which the rate coefficient k_{-1} was obtained from the slope of the graph as $3{,}4 \times 10^{-5}$ s^{-1}.

To a solution of the [Cp*Ti(N^{Xyl}N){κ^{2}N(2,6-$C_6H_3Me_2$)CPh=CH}] (**10**) (5–50 μmol) and 1,4-dimethoxybenzene (3 mg, internal standard) in benzene-d_6, 20 equiv. 2,6-dimethylaniline (0.1–0.5 mmol) were added at 20 °C. The sample was transferred into a J. Young NMR tube. The tube was transferred to a NMR spectrometer probe that had been pre-cooled to 20 °C. ^{1}H NMR spectra were recorded every 3–5 min for a period of up to 30–50 min. The concentration of the reaction product was plotted against time, and the conversion curve was line-fitted to a first order exponential decay Aexp(−x/b). The initial rate was estimated from −A/b, derived from differentiation of the fitted line for $x = 0$. A plot of the initial rate *versus* the concentration of [Cp*Ti(N^{Xyl}N){κ^{2}N(2,6-$C_6H_3Me_2$)CPh=CH}] (**10**) indicated a linear relationship.

To a solution of [Cp*Ti(N^{Xyl}N){κ^{2}N(2,6-$C_6H_3Me_2$)CPh=CH}] (**10**) (14,8 mg, 25 μmol) and 1,4-dimethoxybenzene (3 mg, internal standard) in benzene-d_6 was added 2,6-dimethylaniline (1–4 μmol) at 20 °C. The sample was transferred into a J. Young NMR tube. The tube was transferred to a NMR spectrometer probe that had been pre-cooled to 20 °C. ^{1}H NMR spectra were recorded every 5 min for a period of up to 60 min and then every 10 min for another hour. The reaction product was plotted against time, and the conversion curve was line-fitted to a first order exponential decay Aexp(−x/b). The initial rate was estimated from −A/b, derived from differentiation of the fitted line for $x = 0$. A plot of the initial rate *versus* the concentration of 2,6-dimethylaniline indicated a linear relationship. The *pseudo*-first order rate coefficient was obtained from the slope of the line and the second order rate coefficient k_2 was obtained from $k_2' = k_2 \times$ [MC] as 1.58×10^{-3} L mol^{-1} s^{-1}.

(C) General method for intermolecular hydroaminations

A Schlenk tube equipped with a Teflon stopcock and a magnetic stirring bar was charged with the alkyne (2.40 mmol), the amine (2.40 mmol), the catalyst (0.12 mmol, 5 mol%) and toluene (1 mL). The resulting mixture was heated to 105 °C for 24 h. Then the mixture was cooled to room temperature and a mixture of $NaBH_3CN$ (4.80 mmol) and $ZnCl_2$ (2.4 mmol) in methanol (10 mL) was added. After this mixture had been stirred at 25 °C for at least 20 h, dichloromethane and a saturated aqueous solution of Na_2CO_3 were added. The mixture was filtered and the solid residue was washed with dichloromethane. After extraction, the organic phase was separated. The aqueous layer was extracted with dichloromethane and the combined organic layers were dried over Na_2SO_4. After concentration under vacuum, the residue was purified by flash chromatography (light petroleum ether/EtOAc/SiO_2).

(D) General method for intramolecular hydroaminations

An oven dried Schlenk tube equipped with a Teflon valve stopcock and a magnetic stirring bar was transferred into a nitrogen filled glovebox and charged with the catalyst (0.12 mmol, 5 mol%). The aminoalkyne (2.4 mmol) was subsequently added and the mixture was dissolved in toluene (1 mL). The resulting solution was heated for 6 h at 105 °C. The mixture was allowed to reach room temperature before a mixture of $NaCNBH_3$ (4.8 mmol), $ZnCl_2$ (2.4 mmol) and methanol (10 mL) was added. The mixture was stirred at room temperature for 20 h. Then dichloromethane and a saturated aqueous solution of Na_2CO_3 were added. After filtration the residue was washed with dichloromethane. The organic layer was separated and the aqueous layer was extracted with dichloromethane. The combined organic layers were dried over $MgSO_4$ and the solvent was removed under reduced pressure. The resulting product was purified by flash chromatography (EtOAc/3% NH_3 in MeOH/SiO_2).

(E) Computational study

All calculations were performed on the Gaussian 03 suite of programs.[28] Calculations were carried out using the hybrid B3PW91 functional, with the 6–31G(d,p) basis set for all atoms. Geometry optimisations were initially performed without geometry restraints, followed by frequency calculations to ascertain the nature of the resulting structure (minimum *vs.* transition state). Attempts to determine the corresponding structures for the real (non-simplified) ligands were successful for the reaction products, and gave structures which were comparable to the simplified structures; however calculation of the transition states with the non-simplified systems lead to multiple-order saddle points; single, well-defined transition states were not located.

(F) X-Ray crystal structure determinations

Crystal data and details of the structure determinations are listed in Table 7. Intensity data were collected at low temperature with an Enraf-Nonius Kappa CCD (complex **1**) and a Bruker AXS Smart 1000 CCD diffractometer (MoKα radiation, graphite monochromator, $\lambda = 0.71073$ Å). Data were corrected for air and detector absorption, Lorentz and polarization effects;[29,30] absorption by the crystal was treated with a semiempirical multi-scan method.[31,32] The structures were solved by the heavy atom method combined with structure expansion by direct methods applied to difference structure factors[33] or by conventional direct methods[34,35] and refined by full-matrix least squares methods

Table 7 Details of the crystal structure determinations of the complexes **1**, **3**, **4**, **5** and **11**

	1	**3**	**4**	**5**	**11**
Empirical formula	$C_{24}H_{36}N_2Ti$	$C_{31}H_{41}N_3Ti$	$C_{34}H_{47}N_3Ti$	$C_{30}H_{39}N_3Ti$	$C_{44}H_{59}N_3Ti$
M_r	400.45	503.57	545.65	489.54	677.84
T/K	193(2)	100(2)	100(2)	100(2)	100(2)
λ/Å	0.71073	0.71073	0.71073	0.71073	0.71073
Crystal system	Triclinic	Monoclinic	Triclinic	Monoclinic	Triclinic
Space group	$P\bar{1}$	$C2/c$	$P\bar{1}$	$P2_1/c$	$P\bar{1}$
a/Å	8.6070(17)	17.143(2)	8.0565(4)	13.8833(13)	9.509(2)
b/Å	9.2070(18)	25.0707(3)	10.2565(5)	9.7449(9)	12.983(3)
c/Å	15.015(3)	14.581(2)	18.9495(10)	20.1013(18)	17.624(4)
α/°	91.00(3)	90	86.2970(10)	90	105.994(4)
β/°	100.98(3)	116.658(2)	84.8290(10)	100.422(2)	96.108(4)
γ/°	106.19(3)	90	79.4270(10)	90	108.513(4)
V/Å^3	1118.6(4)	5600.4(12)	1531.13(13)	2674.7 (4)	1937.9(7)
Z	2	8	2	4	2
D_c/Mg m^{-3}	1.189	1.194	1.184	1.216	1.162
μ(MoKα)/mm^{-1}	0.393	0.329	0.306	0.342	0.254
F_{000}	432	2160	588	1048	732
Crystal size/mm^3	0.4 × 0.35 × 0.20	0.40 × 0.10 × 0.10	0.30 × 0.25 × 0.20	0.10 × 0.10 × 0.10	0.15 × 0.15 × 0.05
θ range/°	2.3–30.6	2.3–30.0	2.0–31.0	2.1–25.0	1.8–30.0
Index ranges (indep. set) h,k,l	$-12 \le h \le 11$, $-13 \le k \le 13$, $0 \le l \le 21$	$-24 \le h \le 21$, $0 \le k \le 35$, $0 \le l \le 20$	$-11 \le h \le 11$, $-14 \le k \le 14$, $0 \le l \le 27$	$-16 \le h \le 16$, $0 \le k \le 11$, $0 \le l \le 23$	$-13 \le h \le 13$, $-18 \le k \le 17$, $0 \le l \le 24$
Reflections measured	31 528	57 812	37 750	35 562	45 869
Unique [R_{int}]	6832 [0.0224]	8193 [0.0537]	9660 [0.0453]	4724 [0.0916]	11 314 [0.0547]
Max., min. transmission factors	0.9095, 0.8347	0.7464, 0.5941	0.7464, 0.6805	0.7463, 0.6577	0.7464, 0.6762
Data/restraints/parameters	6832/0/253	8193/0/326	9660/0/354	4724/0/316	11 314/9/455
GOF on F^2	1.053	1.031	1.079	1.078	1.112
R indices [$F > 4\sigma(F)$] $R(F)$, w$R(F^2)$	0.0397, 0.0991	0.0398, 0.0930	0.0436, 0.1168	0.0525, 0.1140	0.0563, 0.1461
R indices (all data) $R(F)$, w$R(F^2)$	0.0494, 0.1036	0.0680, 0.1136	0.0606, 0.1255	0.1078, 0.1490	0.0869, 0.1588
Largest residual peaks/e Å^{-3}	0.364 and –0.365	0.0501 and –0.397	0.473 and –0.366	0.455 and –0.432	0.932 and –0.548

based on F^2 against all unique reflections.[35,36] All non-hydrogen atoms were given anisotropic displacement parameters. Hydrogen atoms were input at calculated positions and refined with a riding model. The C_4N ring in complex **11** was found disordered between two envelope conformations (refined occupancies 0.65 : 0.35). In the same structure, bond lengths and angles of the solvent of crystallization (pentane) had to be restricted to sensible values due to severe disorder effects.

Acknowledgements

We thank the Deutsche Forschungsgemeinschaft (SFB 623) for funding.

References

1 (*a*) Reviews: I. A. Chekulaeva and L. V. Kondratjeva, *Russ. Chem. Rev.*, 1965, **34**, 669; (*b*) D. Steinborn and R. Taube, *Z. Chem.*, 1986, **26**, 349; (*c*) R. Taube, in *Applied Homogeneous Catalysis with Organometallic Compounds*, ed. B. Cornils and W. A. Herrmann, VCH, Weinheim, 1996, 507; (*d*) T. E. Müller and M. Beller, *Chem. Rev.*, 1998, **98**, 675; (*e*) T. E. Müller, M. Beller, in *Transition Metals for Organic Synthesis*, ed. M. Beller and C. Bolm, Wiley-VCH, Weinheim, 1998, vol. 2, 316; (*f*) E. Haak and S. Doye, *Chem. Unserer. Zeit*, 1999, **33**, 296; (*g*) M. Nobis and B. Drießen-Hölscher, *Angew. Chem., Int. Ed.*, 2001, **40**, 3983; (*h*) J. J. Brunet, D. Neibecker, in *Catalytic Heterofunctionalization*, ed. A. Togni and H. Grützmacher, Wiley-VCH, Weinheim, 2001, 91; (*i*) P. W. Roesky and T. E. Müller, *Angew. Chem., Int. Ed.*, 2003, **42**, 2708; (*j*) F. Pohlki and S. Doye, *Chem. Soc. Rev.*, 2003, **32**, 104; (*k*) I. Bytschkov and S. Doye, *Eur. J. Org. Chem.*, 2003, 935; (*l*) J. F. Hartwig, *Pure Appl. Chem.*, 2004, **76**, 507; (*m*) F. Alonso, I. P. Beletskaya and M. Yus, *Chem. Rev.*, 2004, **104**, 3079; (*n*) S. Doye, *Synlett*, 2004, 1653; (*o*) A. L. Odom, *Dalton Trans.*, 2005, 225; (*p*) K. C. Hultzsch, *Adv. Synth. Catal.*, 2005, **347**, 367; (*q*) K. C. Hultzsch, *Org. Biomol. Chem.*, 2005, **3**, 1819; (*r*) R. Severin and S. Doye, *Chem. Soc. Rev.*, 2007, **36**, 1407; (*s*) T. E. Müller, K. C. Hultzsch, M. Yus, F. Foubelo and M. Tada, *Chem. Rev.*, 2008, **108**, 3795; (*t*) J.-J. Brunet and N.-C. Rodriguez-Zubiri, *Eur. J. Inorg. Chem.*, 2007, 4711.

2 (*a*) I. Bytschkov and S. Doye, *Tetrahedron Lett.*, 2001, **43**, 3715; (*b*) I. Bytschkov, H. Sibeneicher and S. Doye, *Eur. J. Org. Chem.*, 2003, 2888; (*c*) C. Li, R. K. Thomson, B. Gillon, B. O. Patrick and L. L. Schafer, *Chem. Commun.*, 2003, 2462.

3 (*a*) L. Ackermann and R. G. Bergman, *Org. Lett.*, 2002, **4**, 1475; (*b*) L. Ackermann and R. G. Bergman, *J. Am. Chem. Soc.*, 2003, **125**, 11956; (*c*) J. M. Hoover, J. R. Petersen, J. H. Pikul and A. R. Johnson, *Organometallics*, 2004, **23**, 4614; (*d*) R. O. Ayinla and L. L. Schafer, *Inorg. Chim. Acta*, 2006, **359**, 3097.

4 (*a*) J. A. Bexrud, J. D. Beard, D. C. Leitch and L. L. Schafer, *Org. Lett.*, 2005, **7**, 1959; (*b*) H. Kim, P. H. Lee and T. Livinghouse, *Chem. Commun.*, 2005, 5205; (*c*) C. Müller, C. Loos, N. Schulenberg and S. Doye, *Eur. J. Org. Chem.*, 2006, 2499; (*d*) R. K. Thomson, J. A. Bexrud and L. L. Schafer, *Organometallics*, 2006, **25**, 4069; (*e*) D. A. Watson, M. Chiu and R. G. Bergman, *Organometallics*, 2006, **25**, 4731; (*f*) A. V. Lee and L. L. Schafer, *Organometallics*, 2006, **25**, 5249; (*g*) H. Kim, Y. K. Kim, J. H. Shim, M. Kim, M. Han, T. Livinghouse and P. H. Lee, *Adv. Synth. Catal.*, 2006, **348**, 2609; (*h*) M. C. Wood, D. C. Leitch, C. S. Yeung, J. A. Kozak and L. L. Schafer, *Angew. Chem., Int. Ed.*, 2007, **46**, 354; (*i*) B. D. Stubbert and T. J. Marks, *J. Am. Chem. Soc.*, 2007, **129**, 6149; (*j*) K. Marcsekova and S. Doye, *Synlett*, 2007, 2564; (*k*) J. A. Bexrud, C. Li and L. L. Schafer, *Organometallics*, 2007, **26**, 6366; (*l*) C. Müller, W. Saak and S. Doye, *Eur. J. Org. Chem.*, 2008, 2731; (*m*) S. Majumder and A. L. Odom, *Organometallics*, 2008, **27**, 1174; (*n*) A. L. Gott, A. J. Clarke, G. J. Clarkeson and P. Scott, *Chem. Commun.*, 2008, 1422.

5 (*a*) Selected examples: E. Haak and S. Doye, *DE 19913522; Chem. Abstr.*, 2000, **133**, 266588; (*b*) E. Haak, I. Bytschkov and S. Doye, *Angew. Chem., Int. Ed.*, 1999, **38**, 3389; (*c*) E. Haak, H. Siebeneicher and S. Doye, *Org. Lett.*, 2000, **2**, 1935; (*d*) A. Heutling and S. Doye, *J. Org. Chem.*, 2002, **67**, 1961; (*e*) F. Pohlki, A. Heutling, I. Bytschkov, T. Hotopp and S. Doye, *Synlett*, 2002, 799; (*f*) A. Heutling, F. Pohlki and S. Doye, *Chem.–Eur. J.*, 2004, **10**, 3059; (*g*) A. Tillack, I. Garcia Castro, C. G. Hartung and M. Beller, *Angew. Chem., Int. Ed.*, 2002, **41**, 2541; (*h*) A. Tillack, H. Jiao, I. Garcia Castro, C. G. Hartung and M. Beller, *Chem.–Eur. J.*, 2004, **10**, 2409; (*i*) A. Tillack, V. Khedkar, H. Jiao and M. Beller, *Eur. J. Org. Chem.*, 2005, 5001; (*j*) Z. Zhang and L. L. Schafer, *Org. Lett.*, 2003, **5**, 4733; (*k*) C. Cao, J. T. Ciszewski and A. L. Odom, *Organometallics*, 2001, **20**, 5011; (*l*) Y. Shi, C. Hall, J. T. Ciszewski, C. Cao and A. L. Odom, *Chem. Commun.*, 2003, 586; (*m*) D. L. Swartz II and A. L. Odom, *Organometallics*, 2006, **25**, 6125; (*n*) M. A. Esteruelas, A. M. López, A. C. Mateo and E. Onate, *Organometallics*, 2005, **24**, 5084; (*o*) M. L. Buil, M. A. Esteruelas, A. M. López and A. C. Mateo, *Organometallics*, 2006, **25**, 4079; (*p*) M. L. Buil, M. A. Esteruelas, A. M. López, A. C. Mateo and E. Onate, *Organometallics*, 2007, **26**, 554.

6 J. S. Johnson and R. G. Bergman, *J. Am. Chem. Soc.*, 2001, **123**, 2923.

7 with a few exceptions:B. D. Stubbert and T. J. Marks, *J. Am. Chem. Soc.*, 2007, **129**, 6149.

8 (*a*) P. D. Knight, I. Munslow, P. N. O'Shaughnessy and P. Scott, *Chem. Commun.*, 2004, 894; (*b*) D. V. Gribkov and K. C. Hultzsch, *Angew. Chem., Int. Ed.*, 2004, **43**, 5542.

9 (*a*) F. Pohlki and S. Doye, *Angew. Chem., Int. Ed.*, 2001, **40**, 2305; (*b*) B. F. Straub and R. G. Bergman, *Angew. Chem., Int. Ed.*, 2001, **40**, 4632.

10 (*a*) P. J. Walsh, A. M. Baranger and R. G. Bergman, *J. Am. Chem. Soc.*, 1992, **114**, 1708; (*b*) A. M. Baranger, P. J. Walsh and R. G. Bergman, *J. Am. Chem. Soc.*, 1993, **115**, 2753.

11 (*a*) M. E. G. Skinner and P. Mountford, *J. Chem. Soc., Dalton Trans.*, 2002, 1694; (*b*) J. R. Hagadorn and J. Arnold, *Organometallics*, 1996, **15**, 984; (*c*) F. T. Edelmann and J. Richter, *Eur. J. Solid State Inorg. Chem.*, 1996, **33**, 157; (*d*) S. Bambirra, M. W. Bouwkamp, A. Meetsma and B. Hessen, *J. Am. Chem. Soc.*, 2004, **126**, 9182.

12 (*a*) Examples:Y. Zhang, E. K. Reeder, R. J. Keaton and L. R. Sita, *Organometallics*, 2004, **23**, 3512; (*b*) Y. Zhang and L. R. Sita, *Chem. Commun.*, 2003, 2358; (*c*) K. C. Jayaratne, R. J. Keaton, D. A. Henningsen and L. R. Sita, *J. Am. Chem. Soc.*, 2000, **122**, 10490; (*d*) A. Littke, N. Sleiman, C. Bensimon, D. S. Richeson, G. P. A. Yap and S. J. Brown, *Organometallics*, 1998, **17**, 446; (*e*) R. J. Keaton, K. C. Jayaratne, D. A. Henningsen, L. A. Koterwas and L. R. Sita, *J. Am. Chem. Soc.*, 2001, **123**, 6197; (*f*) C. Li, R. K. Thomson, B. Gillon, B. O. Patrick and L. L. Schafer, *Chem. Commun.*, 2003, 2462; (*g*) D. A. Kissounko, Y. Zhang, M. B. Harney and L. R. Sita, *Adv. Synth. Catal.*, 2004, **347**, 426; (*h*) C. L. Boyd, E. Clot, A. E. Guiducci and P. Mountford, *Organometallics*, 2005, **24**, 2347; (*i*) A. E. Guiducci, A. R. Cowley, M. E. G. Skinner and P. Mountford, *J. Chem. Soc., Dalton Trans.*, 2001, 1392.

13 E. A. Brussee, A. Meetsma, B. Hessen and J. H. Teuben, *Chem. Commun.*, 2000, 497.

14 B. D. Ward, H. Risler, K. Weitershaus, S. Bellemin-Laponnaz, H. Wadepohl and L. H. Gade, *Inorg. Chem.*, 2006, **45**, 7777.

15 (*a*) L. R. Sita and J. R. Babcock, *Organometallics*, 1998, **17**, 5228; (*b*) L. A. Koterwas, J. C. Fettinger and L. R. Sita, *Organometallics*, 1999, **18**, 4183; (*c*) L. R. Sita, J. R. Babcock, F. P. Arnold, M. Lam, K.-C. Lam, C. D. Incarvito, and A. L. Reingold, *Book of Abstracts, 217th ACS National Meeting, Anaheim*, 1999, INOR-643.

16 (*a*) F. H. Allen and O. Kennard, *Chem. Des. Automat. News*, 1993, **8**, 1 and 31; (*b*) D. A. Fletcher, R. F. McMeeking and D. J. Parkin, *J. Chem. Inf. Comput. Sci.*, 1996, **36**, 746.

17 (*a*) A. J. Blake, P. E. Collier, L. H. Gade, P. Mountford, J. Lloyd, S. M. Pugh, M. Schubart, M. E. G. Skinner and D. J. M. Trösch, *Inorg. Chem.*, 2001, **40**, 870; (*b*) A. J. Blake, G. I. Nikonov and P. Mountford, *Acta Crystallogr., Sect. C: Cryst. Struct. Commun.*, 1997, **53**, 874; (*c*) S. M. Pugh, D. J. M. Trösch, D. J. Wilson, A. Bashall, F. G. N. Cloke, L. H. Gade, P. B. Hitchcock, M. McPartlin, J. F. Nixon and P. Mountford, *Organometallics*, 2000, **19**, 3205.

18 A. J. Blake, P. E. Collier, S. C. Dunn, W.-S. Li, P. Mountford and O. V. Shishkin, *J. Chem. Soc., Dalton Trans.*, 1997, 1549.

19 A. E. Guiducci, C. L. Boyd and P. Mountford, *Organometallics*, 2006, **25**, 1167.

20 N. Vujkovic, B. D. Ward, A. Maisse-Francois, H. Wadepohl, P. Mountford and L. H. Gade, *Organometallics*, 2007, **26**, 5522.

21 J. L. Polse, R. A. Andersen and R. G. Bergman, *J. Am. Chem. Soc.*, 1998, **120**, 13405.

22 D. J. M. Trösch, P. E. Collier, A. Bashall, L. H. Gade, M. McPartlin, P. Mountford and S. Radojevic, *Organometallics*, 2001, **20**, 3308.

23 (*a*) C. C. Cummins, C. P. Schaller, G. D. Vanduyne, P. T. Wolczanski, A. W. E. Chan and R. Hoffmann, *J. Am. Chem. Soc.*, 1991, **113**, 2985; (*b*) J. L. Bennett and P. T. Wolczanski, *J. Am. Chem. Soc.*, 1997, **119**, 10696; (*c*) C. P. Schaller, C. C. Cummins and P. T. Wolczanski, *J. Am. Chem. Soc.*, 1996, **118**, 591; (*d*) C. P. Schaller, J. B. Bonanno and P. T. Wolczanski, *J. Am. Chem. Soc.*, 1994, **116**, 4133; (*e*) J. L. Bennett and P. T. Wolczanski, *J. Am. Chem. Soc.*, 1994, **116**, 2179; (*f*) C. C. Cummins, S. M. Baxter and P. T. Wolczanski, *J. Am. Chem. Soc.*, 1988, **110**, 8731.

24 (*a*) H. M. Hoyt and R. G. Bergman, *Angew. Chem., Int. Ed.*, 2007, **46**, 5580; (*b*) H. M. Hoyt, F. E. Michael and R. G. Bergman, *J. Am. Chem. Soc.*, 2004, **126**, 1018; (*c*) S. Y. Lee and R. G. Bergman, *J. Am. Chem. Soc.*, 1995, **117**, 5877; (*d*) P. J. Walsh, F. J. Hollander and R. G. Bergman, *J. Am. Chem. Soc.*, 1988, **110**, 8729.

25 B. D. Ward, A. Maisse-Francois, P. Mountford and L. H. Gade, *Chem. Commun.*, 2004, 704.

26 J. Barker and M. Kilner, *Coord. Chem. Rev.*, 1994, **133**, 219.

27 H. Yamamoto, H. Yasuda, K. Tatsumi, K. Lee, A. Nakamura, J. Chen, Y. Kai and N. Kasai, *Organometallics*, 1989, **8**, 105.

28 M. J. Frisch, G. W. Trucks, H. B. Schlegel, G. E. Scuseria, M. A. Robb, J. R. Cheeseman, V. G. Zakrzewski, J. J. A. Montgomery, R. E. Stratmann, J. C. Burant, S. Dapprich, J. M. Millam, A. D. Daniels, K. N. Kudin, M. C. Strain, O. Farkas, J. Tomasi, V. Barone, M. Cossi, R. Cammi, B. Mennucci, C. Pomelli, C. Adamo, S. Clifford, J. Ochterski, G. A. Petersson, P. Y. Ayala, Q. Cui, K. Morokuma, D. K. Malick, A. D. Rabuck, K. Raghavachari, J. B. Foresman, J. Cioslowski, J. V. Ortiz, A. G. Baboul, B. B. Stefanov, G. Liu, A. Liashenko, Y. Piskorz, A. Nanayakkara, C. Gonzalez, M. Challacombe, P. M. W. Gill, B. Johnson, W. Chen, M. W. Wong, J. L. Andres, M. Head-Gordon, E. S. Replogle, and J. A. Pople, in *Gaussian 03, Revision B.03*, 2003.

29 Z. Otwinowski, W. Minor, in HKL, *Methods of Enzymology*, ed. C. W. Carter, Jr. and R. M. Sweet, 1997, vol. 276, p. 307.

30 *SAINT*, Bruker AXS, 2007.

31 R. H. Blessing, *Acta Crystallogr., Sect. A: Found. Crystallogr.*, 1995, **51**, 33.

32 G. M. Sheldrick, *SADABS*, Bruker AXS, 2004–2008.

33 P. T. Beurskens, in *Crystallographic Computing 3*, ed. G. M. Sheldrick, C. Krüger and R. Goddard, Clarendon Press, Oxford, UK, 1985, p. 216; P. T. Beurskens, G. Beurskens, R. de Gelder, J. M. M. Smits, S. Garcia-Granda and R. O. Gould, *DIRDIF-2008*, Radboud University, Nijmegen, The Netherlands, 2008.

34 G. M. Sheldrick, *SHELXS-97, Program for solution of crystal structures*, University of Göttingen, Germany, 1997.

35 G. M. Sheldrick, *Acta Crystallogr., Sect. A: Found. Crystallogr.*, 2008, **64**, 112.

36 G. M. Sheldrick, *SHELXL-97, Program for refinement of crystal structures*, University of Göttingen, Germany, 1997.

